DEPARTMENT OF GEOLOGY AND GEOPHYSICS

MASTER
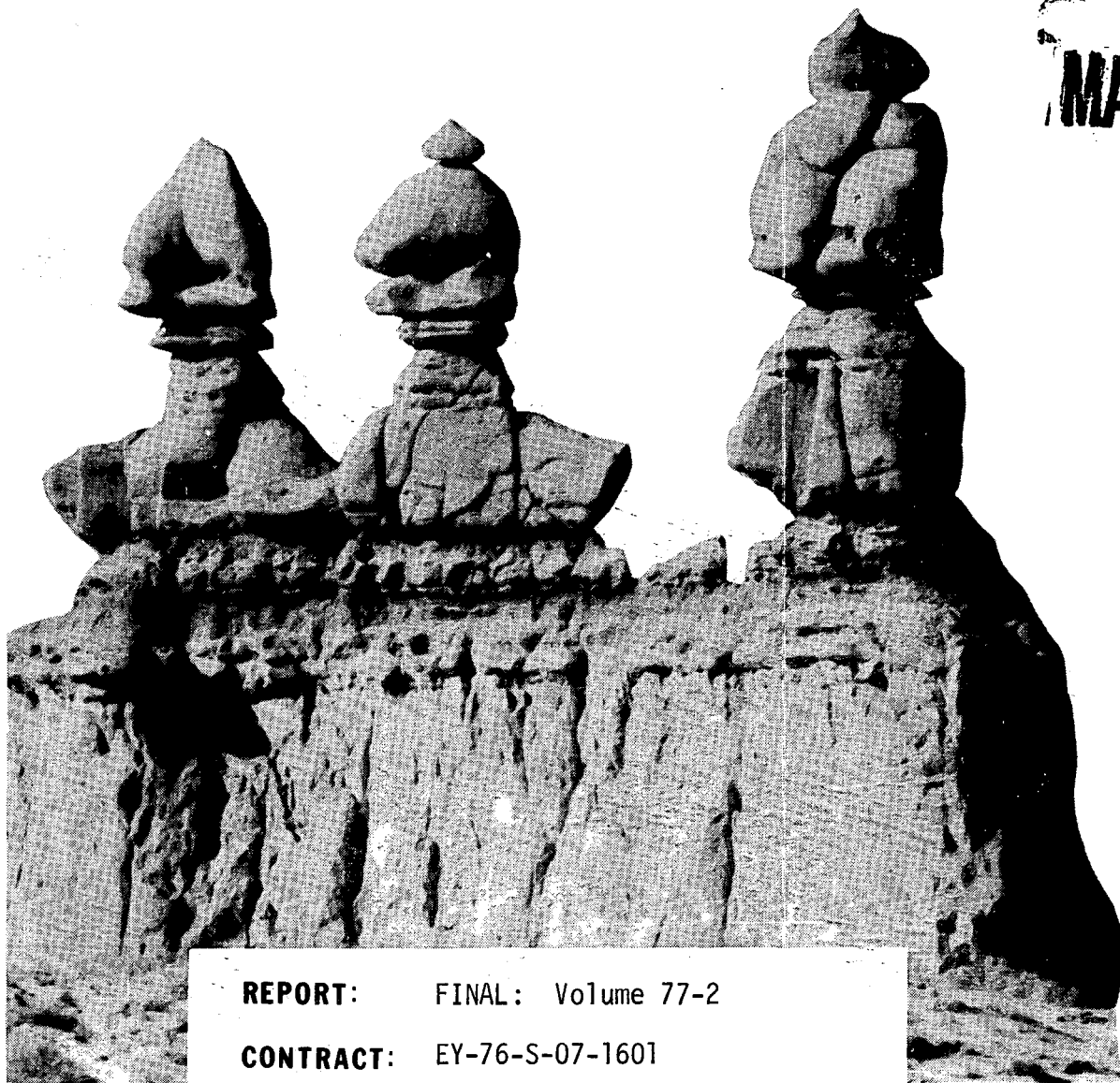
UNIVERSITY OF UTAH   SALT LAKE CITY, UTAH 84112

DISCLAIMER

This report was prepared as an account of work sponsored by an agency of the United States Government. Neither the United States Government nor any agency Thereof, nor any of their employees, makes any warranty, express or implied, or assumes any legal liability or responsibility for the accuracy, completeness, or usefulness of any information, apparatus, product, or process disclosed, or represents that its use would not infringe privately owned rights. Reference herein to any specific commercial product, process, or service by trade name, trademark, manufacturer, or otherwise does not necessarily constitute or imply its endorsement, recommendation, or favoring by the United States Government or any agency thereof. The views and opinions of authors expressed herein do not necessarily state or reflect those of the United States Government or any agency thereof.

DISCLAIMER

Portions of this document may be illegible in electronic image products. Images are produced from the best available original document.

FINAL REPORT: VOLUME 77-2

DOE/DGE

EY-76-S-07-1601

GEOLOGY AND GEOCHEMISTRY OF THE ROOSEVELT

HOT SPRINGS THERMAL AREA, UTAH - A SUMMARY

by

W. T. Parry, W. P. Nash, J. R. Bowman,
S. H. Ward, J. A. Whelan, N. L. Bryant,
R. E. Dedolph, S. H. Evans, D. Bowers

Department of Geology and Geophysics

University of Utah, Salt Lake City, Utah 84112

GEOLOGY AND GEOCHEMISTRY OF THE ROOSEVELT
HOT SPRINGS THERMAL AREA, UTAH - A SUMMARY

W. T. Parry, W. P. Nash, J. R. Bowman, S. H. Ward
J. A. Whelan, N. L. Bryant, R. E. Dedolph, S. H.
Evans, D. Bowers

ABSTRACT

The Roosevelt Hot Springs Thermal Area is a newly discovered geothermal
power prospect. Seven production wells have been drilled with a maximum flow
capability averaging 4.5×10^5 kg of combined vapor and liquid per hour at
a bottom hole temperature of 260°C.

The thermal area is located on the western margin of the Mineral Mountains,
which consist dominantly of a Tertiary granitic pluton 32 km long by 8 km
wide. Rhyolitic tuffs, flows, and domes cover about 25 km^2 of the crest and
west side of the Mineral Mountains within 5 km of the thermal area. The rhyo-
litic volcanism occurred between 0.8 and 0.5 m.y. ago and constitutes a major
Pleistocene thermal event believed to be significant to the evaluation of the
Roosevelt Thermal area. Thermal waters of the dry spring, a seep, and the
deep reservoir are dilute (ionic strength 0.1 to 0.2) sodium chloride brines.

Spring deposits consist of siliceous sinter and minor sulfur. Alluvium
is cemented by sinter and altered in varying degrees by hot, acid-sulfate
water to opal and alunite at the surface, grading successively to alunite-
kaolinite, alunite-kaolinite-montmorillonite, and muscovite-pyrite within 60 m
of the surface. Observed alteration and water chemistry are consistent with

a model in which hot aqueous solutions containing H_2S and sulfate convectively rise along major fractures. Hydrogen sulfide oxidizes to sulfate near the surface decreasing the pH and causes alunite to form. Opal precipitates as the solutions cool. Kaolinite, muscovite, and K-feldspar are formed in sequence, as the thermal water percolates downward and hydrogen ion and sulfate are consumed.

INTRODUCTION

This paper presents a summary of research on the geology and geochemistry of the Roosevelt Hot Springs Thermal Area, located 19 km northeast of Milford, Utah (Fig. 1). A companion paper (Ward and others, this issue) describes the results of geophysical investigations. Discharge from the Roosevelt Hot Springs (Fig. 2) was 38 ℓ/min at 88°C in 1908, 4 ℓ/min at 85°C in 1950, and "small" at 55° in 1957; in 1966 the spring was dry (Mundorff, 1970). A small seep with a temperature of 25°C exists today. Active geothermal exploration began in 1972. Thermal gradient holes were drilled beginning in 1973 and deeper exploration test drilling begun in 1975 resulted in the discovery of a potentially commercial thermal reservoir by Phillips Petroleum Company. The area is currently being explored for commercial power production, and two companies have drilled seven production wells. Flow tests indicate potential production of fluids of about 4.5×10^5 kg/hr per well at a bottom hole temperature of 260°C.

GEOLOGY

The Roosevelt Hot Springs thermal area is situated on the eastern margin of the Basin and Range province in an area where igneous activity has occured

repeatedly during the past 30 m.y. Late Cenozoic volcanism is common along

the edge of the Basin and Range physiographic province in Utah, and the

Roosevelt area is one of four Known Geothermal Resource Areas (KGRA's) there

(Fig. 1). The rock types associated with these KGRA's are high silica

rhyolite and basalt or basaltic andesite, the bimodal association character-

istic of the province in the late Cenozoic.

The Roosevelt Hot Springs thermal area is located on the western margin

of the Mineral Mountains, a Basin-Range horst, composed of the granitic

Mineral Mountains pluton, Precambrian metamorphic rocks, Cretaceous and Paleo-

zoic sedimentary rocks, Tertiary volcanic rocks, and Quaternary rhyolite flows,

domes and ash deposits (Fig. 2). The granitic pluton is the largest in Utah

(approximately 250 km^2) and is no older than 35 m.y. (Lipman and others, 1977).

K-Ar dates of 14 m.y. and 9 m.y. (Armstrong, 1970; Park, 1970) probably re-

sult from reheating during younger igneous events. The dominant unit of the

pluton is a light colored medium to very coarse grained granite, rich in

alkali feldspar and poor in ferromagnesian minerals. In the northern portion

of the area, a hornblende biotite granodiorite predominates. Both types

are gradational to a darker, fine to medium grained granitic unit. The

pluton is cut by mafic and aplitic dikes and porphyritic rhyolite.

Cretaceous, Triassic, and Permian sedimentary rocks are exposed on the

south flank of the pluton, and Cambrian sedimentary rocks are in fault contact

to the north. Precambrian (?) amphibolite-facies schist and gneiss are ex-

posed along the western margin of the pluton.

The Mineral Mountains area has been the site of repeated volcanism.

Mid-Tertiary volcanic activity occurred about 20 m.y. ago, and calc-alkalic

lavas are exposed on the south flank of the Mineral Mountains and in the
Black Mountains which are about 40 km south of the Roosevelt Hot Springs,
adjacent to the Thermo KGRA (Fig. 1). Near the Thermo KGRA, rhyolite dated
at 9.7 m.y. was erupted, and to the north, on the western flank of the
Mineral Mountains, 8.0 m.y. old rhyolite that overlies granitic alluvium de-
rived from the Mineral Mountain pluton is exposed in Corral Canyon. Basalt
dated at 7.6 m.y. occurs on the southern flank of the Mineral Mountains,
near the Minersville Reservoir (Fig. 1) and rhyolite dated at 2.3 m.y. occurs
25 km north of the Roosevelt Hot Springs (Lipman and others, 1977).

The youngest episode of volcanism began about 0.8 m.y. ago with the
eruption of two rhyolite flows from vents located about 4 km east of the
present near-surface thermal activity. These flows, along Bailey Ridge and
Wildhorse Canyon, are about 3 km in length and 80 m thick. The bases of the
flows consist of black flow-layered obsidian, whereas the interior is gray
devitrified rhyolite. Some obsidian is exposed in the upper portion of the
flow. The top consists of perlitic pumice rubble. The rhyolite is almost
entirely glass containing less than 1 percent phenocrysts of alkali feld-
spar, biotite, and Fe-Ti oxides. These flows have reversed magnetic polari-
ties.

Subsequent activity from about 0.6 to 0.5 m.y. ago produced at least
ten rhyolite domes and small flows of rhyolite distributed over 15 km along
the crest and western flank of the Mineral Mountains. The domes range from
about 0.3 to 1 km in diameter and are up to 250 m high. They characteristi-
cally have a basal vitrophyre 5 to 10 m thick which grades upward into a
gray devitrified rhyolite containing abundant lithophysal cavities. On many

of the domes the original frothy perlite carapace is still present. The domes exhibit steeply dipping flow layering and ramp structures which are not present in the more fluid earlier lava flows. The formation of domes was preceded by pyroclastic eruptions which produced air fall and ash-flow tuffs which are best exposed in Ranch Canyon. The dome-forming rhyolites contain up to 10 percent phenocrysts of plagioclase and alkali feldspar, quartz, biotite, Fe-Ti oxides, sphene, zircon, apatite, and allanite. Topaz occurs in lithophysae in crystalline rhyolite. The ash deposits and domes have normal magnetic polarities.

Quaternary basalt was erupted from two vents on the northeast flank of the Mineral Mountains, and flows from the extensive Cove Fort basaltic-andesite field lap against the Mineral Mountains on the east.

Representative chemical analyses indicate that the Quaternary flows and domes are high silica rhyolites (76.5 percent) and contain over 9 percent total alkalies (Table 1). There are chemical differences between the two magma types; the earlier crystal poor flows contain relatively more potassium, titanium, iron, calcium, barium, and strontium, whereas the crystal rich domal rhyolites contain relatively more magnesium, manganese, sodium, fluorine, niobium, and rubidium. The Tertiary rhyolite contains less silica and more calcium, and is strongly enriched in strontium and barium compared to both varieties of Quaternary lavas. One striking feature of the Quaternary lavas is the large compositional range of feldspars precipitated from liquids of similar composition. This is best illustrated by Figure 3 which shows bulk rock and glass compositions together with all the feldspar determinations for both Tertiary and Quaternary rhyolites. If the Tertiary

rhyolite data are deleted (crosses), the feldspar compositional range is not as extensive, but is nevertheless considerable. For the lavas studied here, it is evident that small differences in magma composition, and perhaps temperature, can produce substantial compositional differences in feldspar.

Pre-eruption magma temperatures have been determined using both the iron-titanium oxide and the two-feldspar thermometers. Temperatures range from a high of 785°C in the flows to a low of 650°C in the domes. These temperatures suggest that the magmas contained substantial water and fluorine. Water fugacities calculated for the flows and domes are 3.0 kb and 0.4 kb, respectively (Nash and Evans, 1977).

The chemical and mineralogical data indicate that the dome-forming magma may have been derived from the earlier magma (which gave rise to the flows) by the fractionation of feldspar. The evidence does not preclude the separate generation of each magma batch, or alternatively, derivation of one from the other by chemical gradients as postulated for the Long Valley, California magma system (Hildreth, 1977). The striking chemical similarity of all the domes strongly suggests that they were derived from the same magma batch between 0.6 and 0.5 m.y.

SPRING DEPOSITS AND ALTERATION

Hot spring deposits consist of siliceous sinter and minor sulfur. Thin horizontally bedded, dense, varicolored opaline sinter produced as a result of primary deposition of silica on broad spring aprons occurs in the Opal Mound area. Laminated, knobby, and colloform opal also occur on the Opal Mound. Laminations dip steeply to vertically within old spring vents ex-

posed along the Opal Mound fault. Very porous, cellular opaline sinter occurs in minor amounts on the Opal Mound and north of Hot Springs wash. Sinter-cemented alluvium surrounds the spring vents and constitutes a transition between altered alluvium and spring deposits.

High-grade metamorphic rocks of possible Precambrian age, coarsely crystalline granite to quartz monzonite of Teriary age, and alluvium have been hydrothermally altered in the Roosevelt Hot Springs thermal area (Fig. 2).The alluvium consists of mineral and rock fragments derived from gneiss, granite, and volcanic rocks of the Mineral Range which have been cemented by opal and chalcedony. Feldspars have been altered by acid-sulfate water to alunite, opal, and hematite. Native sulfur occurs as very fine to coarse euhedral to anhedral intergranular crystals. Micro-crystalline sulfur is intergrown with alunite. Cubic pseudomorphs of hematite after pyrite are also present.

Altered rocks have been sampled in three shallow drill holes. Altered and cemented alluvium overlies either altered quartz monzonite or altered gneiss. Very fine grained alunite and opal replace all but quartz grains in alluvium from the granite. Opal lines and fills fractures and intergranular pore spaces. Opal rich zones contain traces of realgar and up to 5% native sulfur. Kaolinite first appears at 9 m to 18 m, montmorillonite at 20 m to 35 m and K-mica at 6 m to 32 m. Jarosite occasionally fills intergranular pore spaces and fractures with traces of barite. Pyrite with marcasite overgrowths are present below the water table at about 32 m. Altered and brecciated gneiss contains varying proportions of bleached, sericitized biotite, K-feldspar, plagioclase, pyrite, marcasite, kaolinite, K-mica, and montmoril-

lonite. Hydrothermal K-feldspar partially replaces a few plagioclase crystals and fills fractures.

Vermiculite, muscovite, clay, and calcite replace biotite in altered quartz monzonite (Fig. 4) in DDH 76-1. Feldspars are replaced by clay, muscovite, calcite, opal, and chalcedony. Veinlets of pyrite, green muscovite, opal, and chalcedony are common. Thin veinlets of K-feldspar-quartz intergrowths are present from 49 m to 61 m. Chemical and modal analyses of altered rocks are shown in Table 2, and abundances of alteration minerals in one shallow core hole (76-1) are shown in Figure 4.

Anomalous concentrations of mercury, arsenic, and lead are associated with the altered rocks. Mercury anomalies as high as 3 ppm are localized over faults in surface rocks. Maximum arsenic in surface rocks is 2,000 ppm near the opal mound, and 430 ppm in altered rocks in drill holes. Maximum lead content of altered rocks is 400 ppm in altered alluvium in one drill hole.

In a simplified thermodynamic model of the alteration, starting materials consist of microcline and a solution similar to the Roosevelt Hot Springs reservoir water. In the model, the dominant reaction process is an exchange of potassium from microcline for hydrogen from solution (Fig. 5). The quantity of microcline consumed per kilogram of solution is a function of temperature and solution pH. Alteration zoning is a function of thermal and pH gradients.

A plausible hypothesis that has been developed for the Steamboat Springs, Nevada thermal system (Schoen and others, 1974) is also applicable for the

development of the surface and near surface alteration at the Roosevelt Hot Springs thermal area. Hot aqueous solutions in equilibrium with K-feldspar, muscovite and quartz, containing H_2S and sulfate convectively rise along major fractures. At the surface, H_2S oxidizes to sulfate decreasing pH and causing alunite to form. Cooling causes opal to precipitate. Low pH, high sulfate, surface water flows away from the fracture and percolates downward. As alunite continues to form, hydrogen ion and sulfate are consumed and kaolinite precipitates as shown in Figure 5. Stability fields for muscovite, and K-feldspar are encountered downward.

WATER CHEMISTRY

Chemical analyses of surface and deep thermal waters are summarized in Table 3. While there is some variability, the analyses indicate that the thermal waters are relatively dilute (ionic strength = .1 to .2) sodium-chloride brines. Sulfate concentrations vary between 48 and 120 mg/l and total dissolved solids are approximately 7,000 mg/l. Chemical differences exist between surface and deep thermal fluid, consisting principally of higher Mg^{++}, Ca^{++}, and $SO_4^=$ and lower Na, K and SiO_2 in surface relative to deep waters. These differences presumably reflect progressive leaching of Mg and Ca by ascending thermal fluids, oxidation of H_2S or admixture of oxidized, $SO_4^=$ rich, surface waters, and flashing and cooling with subsequent precipitation of opal. The Roosevelt Hot Springs thermal fluids are hot-water dominated, in the terminology of White (1970). Thus the Roosevelt Hot Springs geothermal fluids are chemically similar to New Zealand geothermal fluids.

White (1957) described waters that are variously enriched with sodium chloride, H^+, sulfate, and biocarbonate. Within White's definitions, Roose-

velt Hot Springs water could be defined as a sodium chloride water grading into an acid sulfate water. The sulfate measurements of 48-120 mg/l (at Roosevelt) are lower than those at Norris Basin, Yellowstone Park (454 ppm) or Frying Pan Lake, New Zealand (262 ppm) which have been defined as acid-sulfate, chloride waters. Both Na and Cl contents of waters from Roosevelt are considerably higher than for sodium chloride waters described by White (Steamboat Springs, Washoe County, Nevada; Morgan Springs, Tehama County, California; Norris Basin, Yellowstone Park, Wyoming; Well 4 Wairakei, New Zealand).

Application of the Na-K-Ca and SiO_2 thermometers to the seep and the deep geothermal fluid indicates deep water temperatures of 241°C and 286°C, respectively which agree well with deep down-hole measurements. The Na-K-Ca wall-rock equilibration temperature on the Roosevelt seep sample is one of the highest calculated subsurface temperatures in Utah. This high temperature and the presence of extensive surface opal deposits first suggested a viable geothermal resource at Roosevelt Hot Springs.

ACKNOWLEDGMENTS

References

Armstrong, R. L., 1970, Geochronology of Tertiary igneous rocks, eastern Basin and Range Province, western Utah, eastern Nevada, and vicinity, U.S.A.: Geochim. Cosmochim. Acta, v. 34, p. 203-232.

Hildreth, E. W., 1977, The magma Chamber of the Bishop Tuff: Gradients in Temperature, Pressure, and Composition, Unpub. Ph.D. thesis, Univ. Calif., Berkeley, 328 p.

Lipman, P. W., Rowley, D. D., Mehnert, H. H., Evans, S. H., Nash, W. P. and Brown, F. H., 1977, Pleistocene rhyolite of the Mineral Range, Utah: geothermal and archeological significance: Jour. Research U. S. Geol. Survey, in press.

Mundorff, J. C., 1970, Major thermal springs of Utah: Utah Geol. and Mineral Survey Water Resources Bull. 13, 60 p.

Nash, W. P. and Evans, S. H., Jr., 1977, Natural silicic liquids: fugacities and flow: Geol. Soc. America Abstracts with Programs, v. 9, no. 7, p. 1110.

Park, G. M., 1970, Volcanics, Thomas Range: in Radioactive and Isotopic age determinations of Utah Rocks: Utah Geol. and Mineral Survey Bull. 81.

Schoen, R., White, D. E., and Hemley, J. J., 1974, Argillization by descending acid at Steamboat Springs, Nevada: Clays and Clay Minerals, v. 22, p. 1-22.

White, D. E., 1957, Magmatic, connate, and metamorphic waters: Geol. Soc. America Bull., v. 68, p. 1659-1682.

White, D. E., 1970, Geochemistry applied to discovery, evaluation, and exploitation of geothermal energy resources: rapporteur's report: UN Symposium on the Development and Utilization of Geothermal Resources, Pisa Proceedings, (Geothermics, Spec. Iss. 2) v. 1, p. 58-80.

Figure Captions

Figure 1. Distribution of late Tertiary and Quaternary volcanic rocks in west-central Utah. Ages in millions of years. Qb = Quaternary basalt, Qr = Quaternary rhyolite, Tb = Tertiary basalt, Tr = Tertiary rhyolite.

Figure 2. Generalized geologic map of the northern Mineral Mountains, Utah. Quaternary rhyolites are stippled. Bailey Ridge 1, Wildhorse Canyon 2, Corral Canyon 3, Ranch Canyon 4, Opal Mound 5, Bearskin Mountains 6, Little Bearskin Mountain 7, North Twin Flat Mountain 8, South Twin Flat Mountain 9.

Figure 3. Bulk rock (solid symbols) and glass (open symbols) normative compositions plotted in the system albite-orthoclase-quartz. Squares are Quaternary rhyolite, triangles are Tertiary rhyolite of Corral Canyon. The curved line represents the quartz-alkali feldspar boundary a 500 b water pressure. Feldspar compositions in volcanic rocks are shown in the lower triangle. Phenocrysts are solid circles, groundmass are open circles, crosses represent feldspars from Tertiary rhyolite from Corral Canyon. Coexisting feldspars from rhyolite domes are shown by tie lines. Rock and mineral analytical data are tabulated by Evans and Nash (1978).

Figure 4. Abundance of major alteration minerals in DDH 76-1 in weight percent.

Figure 5. Activity diagram of the system $K_2O-Al_2O_3-SiO_2-SO_3-H_2O$ at 100°C and quartz saturation showing one calculated reaction path for microcline and Roosevelt thermal water.

TABLE 2

Chemical* and Modal Analyses of Rocks From the
Roosevelt Thermal Area

Sample No. Description	R9 Sinter	R3 Sinter Cemented Alluvium	DDH 76-1, 4.6 m Sinter cemented acid sulfate altered alluvium	DDH 76-1, 22.9 m Argillized quartz monzonite	DDH 76-1, 47.3 m Weakly propylitized quartz monzonite
SiO_2	91.8	85.9	55.1	76.0	65.6
Al_2O_3	2.6	4.7	17.9	13.9	17.1
TiO_2	0.00	0.08	0.36	0.58	0.71
Fe_2O_3**	0.82	1.0	0.98	0.44	3.
MgO	0.10	0.29	0.37	0.37	0.86
CaO	0.11	0.45	0.34	0.33	1.7
Na_2O	0.10	1.2	n.d.	n.d.	4.0
K_2O	0.09	1.6	3.9	3.8	6.4
L.O.I.***	3.48	3.40	6.60	4.20	0.88
SO_3	0.15	0.07	14.2	0.51	
S					0.15
S≡O					0.08
Total	99.3	98.7	99.8	100.1	100.5

Modal Composition in weight percent

Quartz	94	74	54	48	16
Plagioclase An_{10}	2	12		3	37
K-feldspar	.1	10		23	29
Biotite	.7	2			5
Muscovite				5	10
Alunite	.5	.2	41	0.6	
Kaolinite				16	

Sample No. Description	R9 Sinter	R3 Sinter Cemented Alluvium	DDH 76-1, 15 ft. Sinter cemented acid sulfate altered alluvium	DDH 76-1, 75 ft. Argillized quartz monzonite	DDH 76-1, 155 ft. Weakly propylitized quartz monzonite
Vermiculite			2	2	
Chlorite					1
Pyrite					0.4
Sphene	.2	.3			
Rutile			.4	0.5	0.7
hematite	.7	.7			

*XRF Analysis using Norrish and Hutton method.
**Total iron as Fe_2O_3.
***Loss on ignition less SO_3.

TABLE 3

Selected Roosevelt KGRA Water Analyses

	1	2	3	4
Na	1840	1800	2072	2500
Ca	122	107	31	22
K	274	280	403	488
SiO_2	173	107	639	313
Mg	25	24	.26	0
Cl	3210	3200	3532	4240
SO_4	120	70	48	73
HCO_3	298	300	25	156
Al			1.86	.04
Fe			.016	
Total Dissolved Solids	6063	5888	6752	7792
Temperature	25°C	28°C	92°C	55°C
pH	6.5	6.43	5.0	7.9
Na-K-Ca Temperature	241°C	239°C	274°C	283°C
SiO_2 Temperature	170°C	140°C	283°C	213°C

1) Roosevelt Seep, University of Utah, June, 1975.

2) Roosevelt Seep, Phillips Petroleum Co., August, 1975.

3) Thermal Power Company well 72-16, Univ. of Utah, Jan., 1977. Surface leakage.

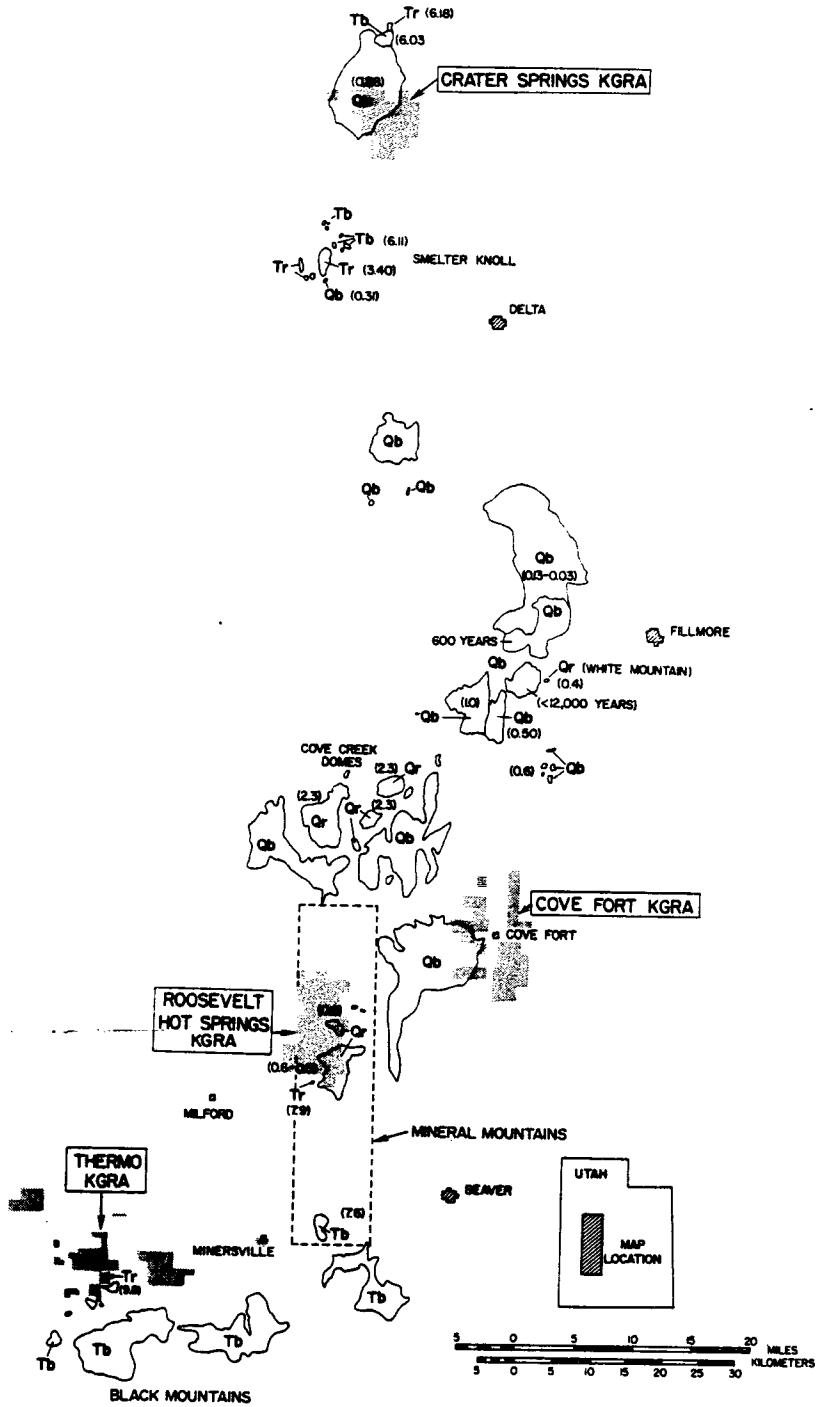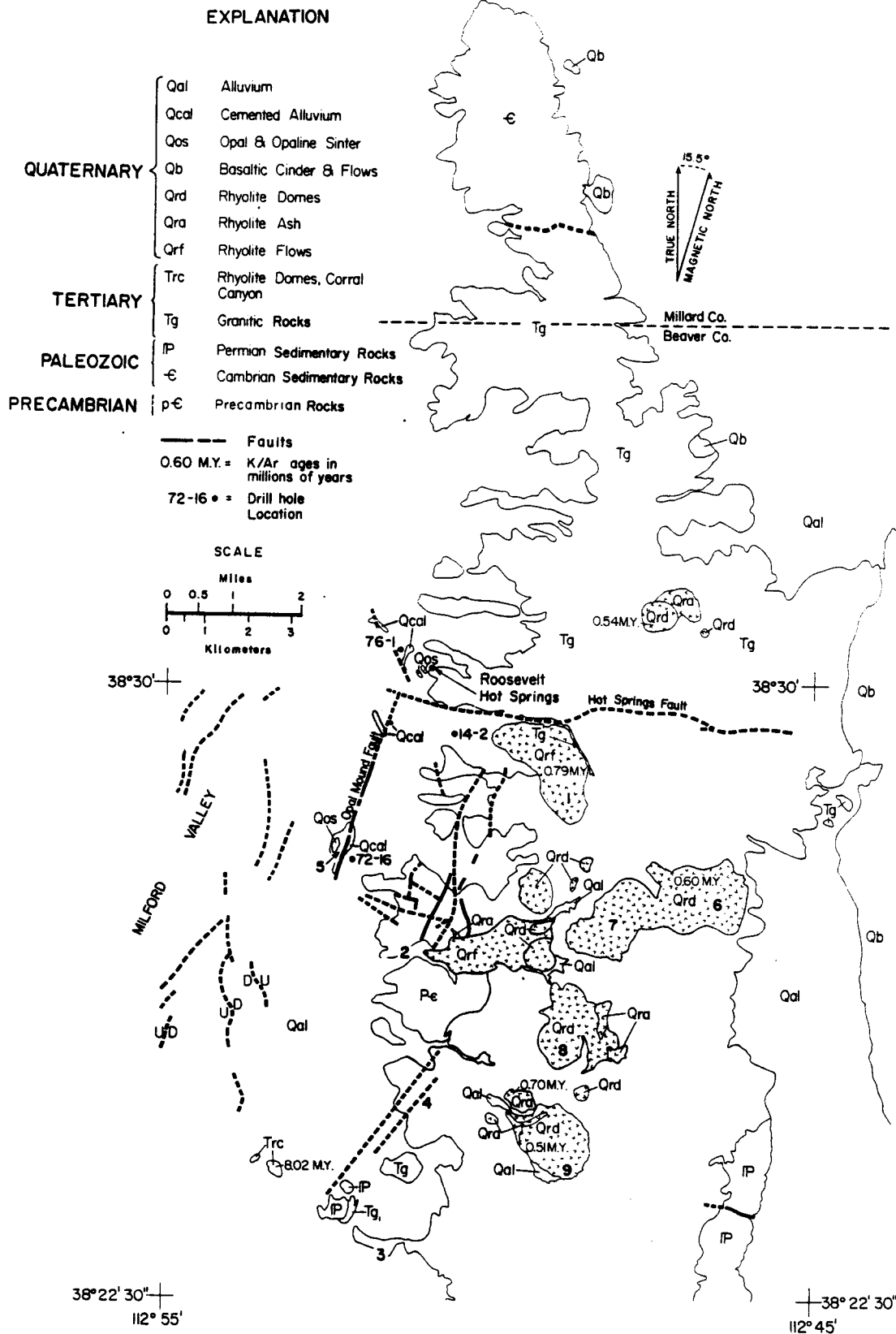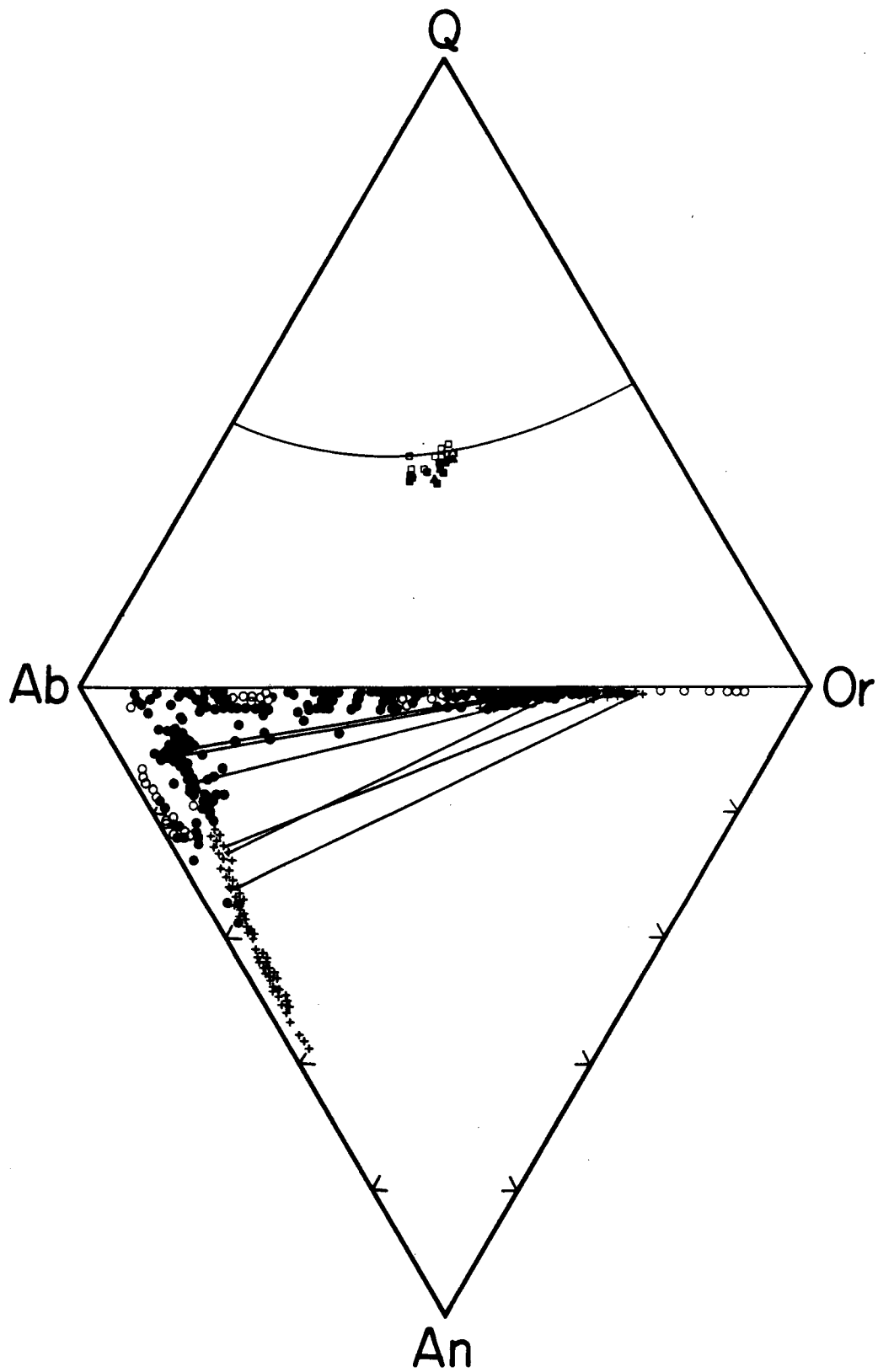4) Roosevelt Hot Springs, Sept., 1957, U.S.G.S., Mundorff (1970).

Figure 1

EXPLANATION

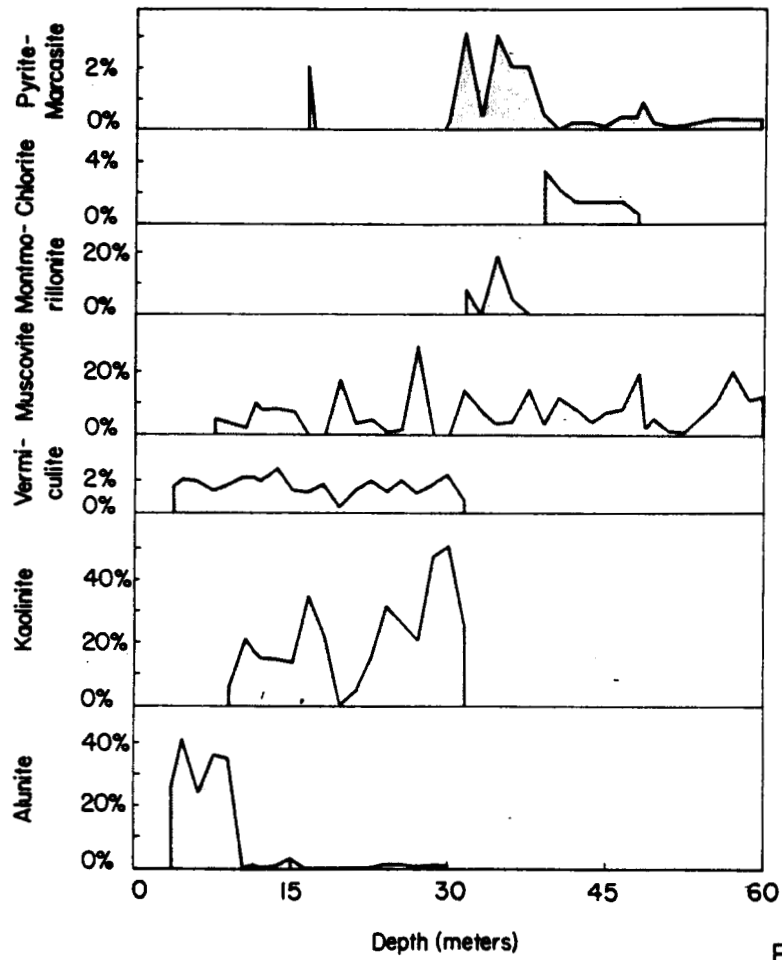QUATERNARY
- Qal — Alluvium
- Qcal — Cemented Alluvium
- Qos — Opal & Opaline Sinter
- Qb — Basaltic Cinder & Flows
- Qrd — Rhyolite Domes
- Qra — Rhyolite Ash
- Qrf — Rhyolite Flows

TERTIARY
- Trc — Rhyolite Domes, Corral Canyon
- Tg — Granitic Rocks

PALEOZOIC
- P — Permian Sedimentary Rocks
- €‌ — Cambrian Sedimentary Rocks

PRECAMBRIAN
- p€‌ — Precambrian Rocks

— — — Faults
0.60 M.Y. = K/Ar ages in millions of years
72-16 • = Drill hole Location

SCALE
Miles
0 0.5 1 2
0 1 2 3
Kilometers

Figure 2

Figure 3

Figure 4

Figure 5

GEOPHYSICS OF THE ROOSEVELT HOT SPRINGS THERMAL AREA, UTAH

by

S. H. Ward, J. M. Bodell, W. D. Brumbaugh, J. A. Carter
K. L. Cook, T. J. Crebs, T. L. Olsen, W. T. Parry, W. R.
Sill, R. B. Smith, I. Thangsuphanich, and A. C. Tripp

Department of Geology and Geophysics

University of Utah, Salt Lake City, Utah 84112

GEOPHYSICS OF THE ROOSEVELT HOT SPRINGS THERMAL AREA, UTAH

ABSTRACT

Minor earthquake activity occurs near the Roosevelt Hot Springs thermal area, Utah, whereas major swarms of earthquakes occur 30 km to the east-northeast near Cove Fort, Utah. Delayed P-wave travel times generated from the Cove Fort microearthquakes, and observed west of the northern Mineral Mountains, are suggestive of a low velocity zone under them; the vertical and lateral resolution of the data is inadequate to delineate the zone. Gravity and magnetic surveys are helpful in understanding the structure and depth of valley fill of the area of the northern Mineral Mountains; on the other hand, neither one has detected, in an obvious manner, an intrusive source of heat. Thermal gradient measurements that range up to 960°C/km in 30 m to 60 m deep holes outline a 6 km by 12 km area which we believe to be reasonably descriptive of the thermal field. Comparison of thermal gradient and resistivity data show that they both outline anomalous zones along the system of faults that control the near-surface fluid flow. The source of both anomalies is interpreted to be the circulation of thermal water, which gives rise to the high heat flow. The lowered resistivity is thought to be due to the hot brine and the associated hydrothermal alteration. Magnetotelluric data are highly anomalous over the field but we have yet to arrive at a means for quantitative interpretation of it.

INTRODUCTION

Numerous geophysical techniques tried at the Roosevelt Hot Springs thermal area, Utah, have helped us to understand the convective hydrothermal system but no one method has been capable of providing unequivocal targets for drilling, nor have the collection of methods unequivocally located the source of heat. Nevertheless, when combined with geological and geochemical data, the sum of the geophysical data sets materially assists in limiting the drilling target. Microearthquakes, gravity, and magnetics have been used to define the regional setting; resistivity and heat flow have been used to localize the convective hydrothermal system; while magnetotellurics, gravity, and magnetics have been used in attempts to locate the source of heat. In interpreting this data we have relied upon the geological and geochemical evidence of Parry et al (this issue).

MICROEARTHQUAKES

Regional seismicity has shown that the Roosevelt Hot Springs and Cove Fort, Utah areas are located where earthquake trends of the north-trending Intermountain Seismic Belt begin to turn east-west across southwestern Utah (Smith and Sbar, 1974). This is a significant tectonic feature because the east-west earthquake trend cross-cuts the north-trending Late Cenozoic horsts and grabens of the eastern Great Basin. The east-west seismic zone may reflect a highly fractured crust that could facilitate magma migration into the upper-crust and thus enhance the geothermal potential.

In 1974 and 1975 earthquake monitoring of both the Roosevelt Hot Springs and Cove Fort areas was conducted as a means of examining the relationships between seismicity and the known geothermal features. The surveys used up to 12 portable, high-gain seismographs (see Fig. 1 for station locations). In 49 days of monitoring, 163 earthquakes of magnitude $-0.5 < M_L < 2.8$ were located. The seismic activity was characterized by shallow-focus earthquakes, most less than 10 km deep. The earthquakes were grouped in three areas: (1) a north-south trend of moderate activity on the west side of Milford Valley, (2) a trend of minor activity along the west side of the Mineral Range, including the Roosevelt Hot Springs thermal area, and (3) an area of numerous swarm-like earthquake sequences around the Cove Fort area. These earthquake data suggest that the Roosevelt Hot Springs thermal area appears to be only slightly active and at a much lower level than the earthquake zones 60 km east near Richfield and Marysvale, Utah. It should be noted that about ten

times more small earthquakes were recorded in the Dog Valley area, six km north of Cove Fort, but were unlocateable because they were not recorded on a sufficient number of stations.

P-wave travel-times, as measured across three stations on the west flank of the Mineral Range (Fig. 1) from earthquakes 30 km away near Cove Fort, showed slight positive delays (later arrivals) of up to 0.2 sec. These delays could have been produced from lateral velocity variations or near-surface low velocity material for which we could not account. Alternatively, they could have been produced by an upper crustal low-velocity layer beneath the Mineral Range. The resolution was not sufficient to delineate the layer.

S-wave delays could not be calculated. However, qualitative estimates of S-wave attenuation at a station south of Roosevelt Hot Springs, from the Cove Fort earthquake sources, suggest a low-Q transmission path. Thus the ray paths that propagate beneath the Mineral Range showed both a low-velocity effect and shear wave attenuation possibly suggestive of a magma source beneath the southern part of the Mineral Range.

Fault-plane solutions (Fig. 1) for the Cove Fort earthquakes demonstrate oblique normal faulting with west to west-northwest directions of the minimum compressive stress. This stress direction is consistent with general east-west extension of the eastern Great Basin that could facilitate emplacement of shallow, crustal magma sources.

The nature of earthquake occurrence at Cove Fort was unusually episodic and demonstrated swarm-type characteristics. A maximum likelihood estimate of b-values at Cove Fort was 0.84 ± 0.16, but values as large as 1.27 ± 0.18 were calculated for the intense swarm activity at Dog Valley. Earthquakes that

occur in volcanic and ocean-spreading settings usually have b-values of 1.0 or greater. Thus the argument for a volcanic relationship of the Cove Fort seismicity can be made. However, the degree of complex faulting at the inter-section of two tectonic trends argues for a locally complex stress field that could produce swarm-type earthquakes and unusually high b-values.

Statistical modeling of the Cove Fort swarms showed a symmetrical dis-tribution of probability energy levels and the general increase in the pro-bability of earthquake occurrence versus energy. These results are similar to those of a published oceanic earthquake swarm (Sykes, 1970). This does not imply a causal relationship, but the statistical modeling and the close spatial association of the Cove Fort-Dog Valley earthquake swarms with the nearby Quaternary basalts suggests that the potential exists for a geo-thermal source related to Holocene volcanism.

GRAVITY AND MAGNETICS

Figure 2 shows the terrain-corrected Bouguer gravity anomaly map based on about 700 stations measured during 1974 through 1976. The generally northward-trending gravity contours with pronounced gradients over the alluvium adjacent to the western margin of the Mineral Mountains, indicate that the mountains are bounded on the west by Basin and Range faults, forming the eastern margin of the Milford Valley graben which is reflected in the gravity low along the western part of the map. Two northward-trending, elongate gravity highs, which are right-laterally offset about 2 km in the intervening area of a gravity saddle in the Ranch Canyon area, extend throughout the central part of Figure 2 (see location A). The northern gravity high overlies principally the western margin of the Mineral Mountains where granitic rocks are exposed; and the elongate gravity spur extending southward from the southern peak of the high (B in Fig. 2) corresponds in a striking manner, both in trend and areal extent, with the pronounced geothermal gradient anomaly (Fig. 6) related to the known geothermal reservoir. The reason for this correspondence is not yet known. Where the Hot Springs Fault (see Fig. 7) intersects the spur, the regularity of the contours are significantly disrupted. The southern gravity high, which extends off the map to the south, overlies the southern part of the Mineral Mountains where Precambrian (?) metamorphic and Paleozoic sedimentary rocks occur. About 2 km north of the Millard-Beaver county line, a fault zone occurs (C of Fig. 2) where the Mineral Mountains pluton terminates against Paleozoic rocks, and the northern gravity high is separated into two separate gravity highs which are right-laterally offset

about 2 km in the intervening area of a gravity saddle. In the southern part of the gravity map (D of Fig. 2) is a pronounced north-northeastward-trending elongate gravity low, about 8 km in length and consisting of two gravity lows (D and E of Fig. 2), that corresponds with a series of volcanic domes, including Bearskin and Little Bearskin Mountains, and North and South Twin Flat Mountains, and which possibly indicates a low-density intrusive at shallow depth (2 km) beneath these volcanic domes.

Figure 3 shows a total magnetic intensity residual anomaly map. The broad northward-trending magnetic high, of about 250 gammas of average total relief, that extends throughout the central part of the map, corresponds with the Mineral Mountains granitic pluton. The small magnetic highs correspond with local areas of increased magnetic susceptibility of both the granitic-type rocks within the pluton and the Precambrian (?) metamorphic rocks that are found both exposed and in drill holes principally along the western margin of the range south of Hot Springs Fault. In the south central part of the map, the striking constriction of the magnetic high anomaly corresponds with (1) a similar constriction of the exposed pluton as a consequence of the previously mentioned volcanic domes which intrude the pluton in this area, (2) a postulated east-west lineament in this area, and (3) the southern end of the pronounced geothermal gradient anomaly (Fig. 6). Near the northern edge of the map (F of Fig. 3) the striking east-west linear trend of the magnetic contours, with a large gradient, corresponds with the northern margin of the Mineral Mountains pluton and the Millard-Beaver county line fault zone. The continuation of the lineament across Milford Valley indicates that the high magnetic susceptibility material (probably granitic) may extend under the alluvium of Milford Valley.

Other magnetic features which correlate well with the geology and/or gravity features are: (1) a magnetic low (G of Fig. 3) which partly overlies the previously mentioned Bearskin and Little Bearskin volcanic domes; (2) an east-west magnetic lineament along the Hot Springs Fault (H of Fig. 3) with a 2-km right-lateral offset of magnetic highs on opposite sides of the fault near the western margin of the Mineral Mountains; and (3) a magnetic low that corresponds almost exactly in areal extent with the reversed magnetic polarity of the Bailey Ridge rhyolite flow (I of Fig. 3).

Figures 4 and 5 show the terrain-corrected Bouguer gravity anomalies and interpretative geologic cross-sections along the east-west line 2.2N and the north-south baseline, respectively. Both lines cross the area of high geothermal gradient (Fig. 6). For these models, the density contrast between the bedrock and alluvium is assumed to be 0.5 gm/cc. The gravity data on line 2.2N (Fig. 4) indicate: (1) the northward-trending Opal Mound horst, which is bounded on the east by the Opal Mound Fault with an indicated vertical displacement of about 50 m; (2) step faults in the bedrock bounding the eastern margin of the Milford Valley graben; and (3) an alluvium thickness of about 1.4 km beneath Milford Valley at the western end of the profile. The gravity data on the baseline (Fig. 5) indicate: (1) the eastward-striking Hot Springs Fault, downthrown on the south, with a vertical displacement of about 65 m; and (2) another eastward-striking fault at 6.5N, downthrown on the north, with a vertical displacement of about 60 m. These two models, based on gravity data, indicate that many pronounced faults, striking both north-south and east-west, occur in the Roosevelt Hot Springs thermal area. Although the area lying east of the Opal Mound Fault and west of the granite outcrop is

modeled along line 2.2N (Fig. 4) with only two faults, the gravity data do not preclude additional faulting and fracturing in this area.

THERMAL MEASUREMENTS

A contoured plan map of shallow (30 m to 60 m) thermal gradients is shown in Figure 6 (after Sill and Bodell, 1977). A comparison of this figure with the lineament map (Fig. 7), shows that the region of highest thermal gradient is aligned along the Opal Mound Fault and Fault 1 in the south, and to the north there is a bending of the contours to the northwest along Fault 5. These alignments and the southern termination of the high thermal gradients by several east-west trending faults demonstrate the fault control on the near-surface circulation.

Comparison of the thermal gradients (Fig. 6) and the 300 m dipole-dipole resistivity data (Fig. 8) show that they both outline anomalous zones along the system of faults that control the near-surface fluid flow. The source of both anomalies is the circulation of thermal water, which gives rise to the high heat flow and to the lowered resistivity due to the hot brine and the associated hydrothermal alteration.

A series of temperature profiles on a west to east line across the system in the southern part was obtained. To the west of the Opal Mound Fault the profiles show a decreasing gradient with increasing depth. The gradients and temperatures increase laterally toward the center of the thermal anomaly and to the east the gradients begin to decrease. The nature of these temperature profiles and the asymmetry of the thermal gradient profile across the system are suggestive of a leakage and mixing of thermal water with the regional groundwater flow to the west.

The maximum conductive heat flow over the anomaly is 40 HFU based on a thermal conductivity of 40 HCU and a maximum thermal gradient of 1000°C/km.

The total conductive heat loss is estimated at 2MW; this is calculated on the basis of an equivalent line source at a depth of 1 km with a strike length of 6.5 km. Heat flow in the Mineral Mountains, to the east of the near-surface thermal anomaly, is lower than the average (2 HFU) for the Basin and Range. This low heat flow suggests that recharge is taking place in this region.

ELECTRICAL MEASUREMENTS

Electrical surveys performed at Roosevelt Hot Springs thermal area include 100 m, 300 m and 1 km dipole-dipole resistivity, Schlumberger resistivity soundings, electromagnetic soundings, and magnetotelluric soundings. The amount of data so recorded has provided an insight into the three-dimensional geolectric section. For example, Figure 8 (after Sill and Ward, 1976) portrays the contours of apparent resistivity observed over the geothermal field in first separation 300 m dipole-dipole resistivity surveying. It represents, we believe, the distribution of brine-soaked clays in the top 500 m of the system. The clays are alteration products of feldspars and occur dominantly along faults and fractures (Fig. 7) in the Tertiary granite host rock. Surface conduction in the kaolinite and montmorillonite secondary clay minerals is estimated to be three times as important as conduction via the high temperature brine existing in the fractures (Sill and Ward, 1976).

Insofar as clay alteration is most dominant along fractures, it is not surprising that the 100 m dipole-dipole survey delineated most of the major fractures of the geothermal field. Figure 7 depicts fractures interpreted from aerial photography (P), observed geology (G), dipole-dipole resistivity surveys (R), and aeromagnetic surveying (M). The density of inferred fractures or faults is greatest where data density is greatest and that occurs in the vicinity of the Opal Mound Fault. Three fracture sets, trending north-northeast, west-northwest, and northwest are in evidence. Further, the granitic terrain is highly fractured leading us to explain the high permeability of the reservoir as fracture-dominated.

When we combine all of the data from the active electrical methods we readily generate the pseudo-geological model of Figure 9. This figure is based on a subjective combination of one-dimensional inverse interpretations of combined Schlumberger and electromagnetic soundings and two-dimensional forward interpretations of both Schlumberger and dipole-dipole data using geological, geochemical, and other geophysical constraints. It is our best model to depths of 500 m for line 3.5N of Figure 8, beyond which the active electrical methods totally lack resolution in this environment.

The apparent resistivities from 25 MT soundings have been inverted to one-dimensional model earths at each sounding site. The resulting model we believe to be a totally unrealistic representation of a subsurface distribution of true resistivities while simultaneously being diagnostic of a convective hydrothermal system. The observed resistivities of less than 1 Ωm at depths of order 2 to 3 km are virtually impossible to obtain unless graphitic horizons or massive sulfides are present; clay alteration should be absent at these depths. Insofar as our current geologic evidence precludes these possibilities, we are inclined to believe that the subsurface resistivities interpreted from the MT data are artifacts of the interpretation technique; two and three-dimensional earth modeling is required to resolve the issue. Meanwhile, we find some comfort in the fact that such strangely low electrical conductivities are frequently found in geothermal environments.

ACKNOWLEDGMENTS

FIGURE CAPTIONS

Figure 1.   Epicenter map of the Roosevelt Hot Springs-Cove Fort, Utah area from earthquake surveys in 1974 and 1975.   Fault plane solutions are lower-hemisphere, equal-area stereographic nets.   Dark areas are quadrants of compression; light areas are quadrants of dilatation.   Arrows indicate directions of minimum compressive stress (T-axes).

Figure 2.   Terrain-corrected/Bouguer gravity anomaly map of the Roosevelt Hot Springs thermal area.   Contour interval = 2 mgal.   Well designations: solid circle--productive well; plain open circle--non-productive well; open circle, with crosses--thermal gradient well.   Letter designations are described in text.

Figure 3.   Total aeromagnetic intensity residual anomaly map of the Roosevelt Hot Springs thermal area.   Contour interval = 50 gammas.   Data taken along east-west lines at 1/4 mile (402 m) spacing drape flown at an elevation of 1,000 feet (305 m) above ground.   International Geophysical Reference Field (IGRF), updated to 1975, removed from data.   Letter designations are described in text.

Figure 4.   Interpretative two-dimensional model for gravity profile along line 2.2N (see Fig. 2) of the Roosevelt Hot Springs thermal area.   Assumed density contrast is 0.5 gm/cc.

Figure 5. Interpretative two-dimensional model for gravity profile along baseline (see Fig. 2) of the Roosevelt Hot Springs thermal area. Assumed density contrast is 0.5 gm/cc.

Figure 6. Plan map of contoured thermal gradients over the Roosevelt Hot Springs thermal area in the depth interval from 30 to 60 m. Contour interval 100°C/km. Also shown are the locations of thermal gradient holes (circle with cross), as well as productive (solid dots) and non-productive (open circle) wells.

Figure 7. Lineaments, interpreted as fractures and faults, mapped by photos (P), geologic observation (G), resistivity survey (R), and aeromagnetic survey (M) over the Roosevelt Hot Springs thermal area. Producing wells shown by solid dots, "dry wells" by open circles, shallow alteration holes by circles with crosses.

Figure 8. Contours of apparent resistivity obtained with dipole-dipole array, first separation, over the Roosevelt Hot Springs thermal area. Contours at 10, 20, 30, 50, 100 ohm-m and multiples of ten times these figures. Productive wells shown by solid dots, "dry wells" by open circles, shallow alteration holes by circles with crosses. Traverse lines are shown.

Figure 9. Pseudo-geologic interpretation of geoelectric section obtained from several electrical surveys along traverse 3.5N (see Fig. 8 for coordinate location) of the Roosevelt Hot Springs thermal area.

References

Parry, W. T., W. P. Nash, J. R. Bowman, S. H. Ward, J. A. Whelan, N. L. Bryant, R. E. Dedolph, S. H. Evans, D. Bowers, 1978, Geology and Geochemistry of the Roosevelt Hot Springs Thermal Area, Utah (this issue).

Sill, W. R., and J. Bodell, 1977, Thermal Gradients and Heat Flow at Roosevelt Hot Springs, Tech. Rept. 77-3, Contract EY-76-S-07-1601, Dept. of Geology and Geophysics, University of Utah.

Sill, W. R., and S. H. Ward, 1976, Dipole-dipole resistivity delineation of the near-surface zone at the Roosevelt Hot Springs Area, Tech. Rept. 76-1, Contract EY-76-S-07-1601, Dept. of Geology and Geophysics, University of Utah.

Smith, R. B., and M. Sbar, 1974, Contemporary Tectonics and Seismicity of the Western States with Emphasis on the Intermountain Seismic Belt: Bull. Geol. Soc. America, vol. 85, p. 1205-1218.

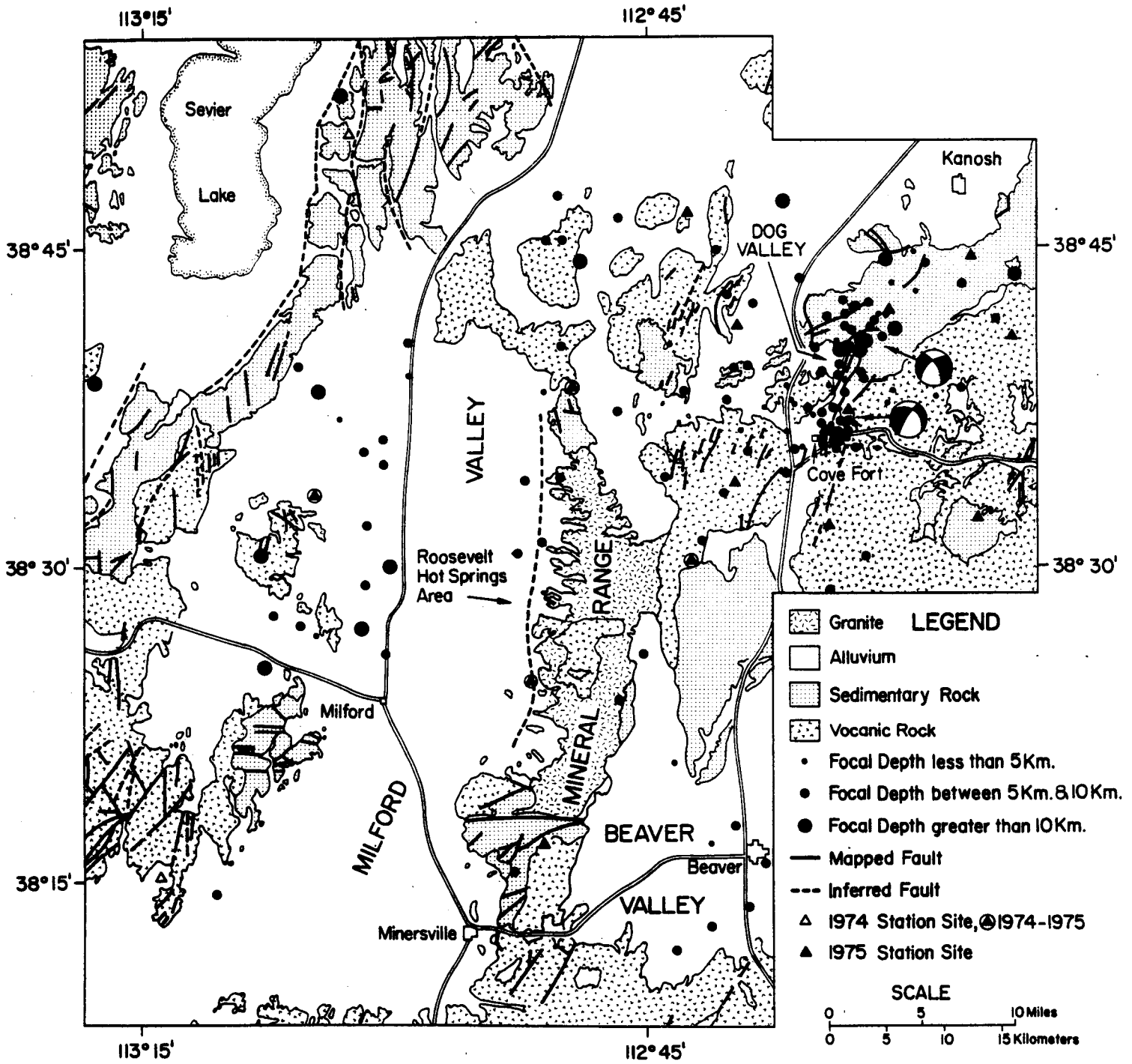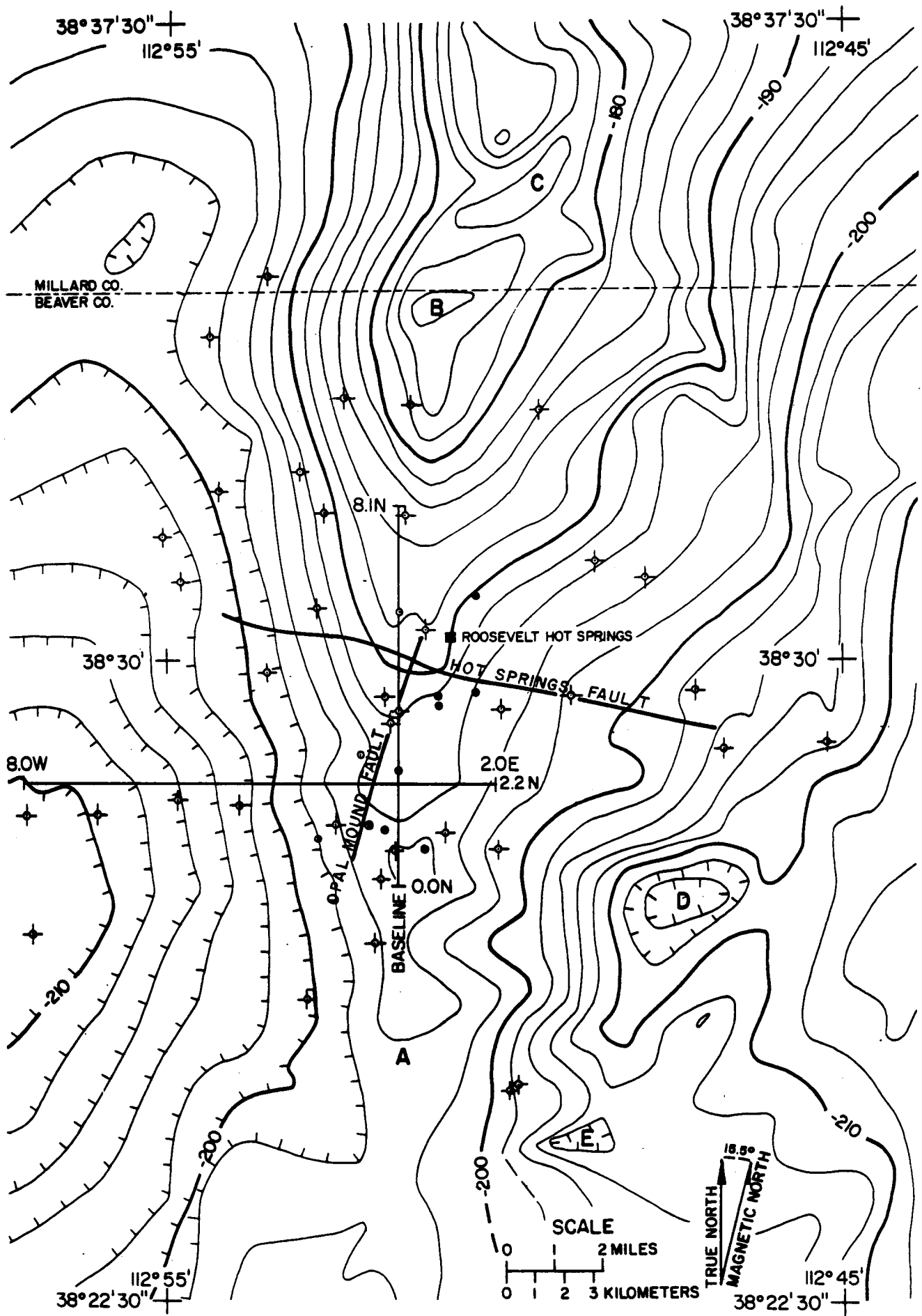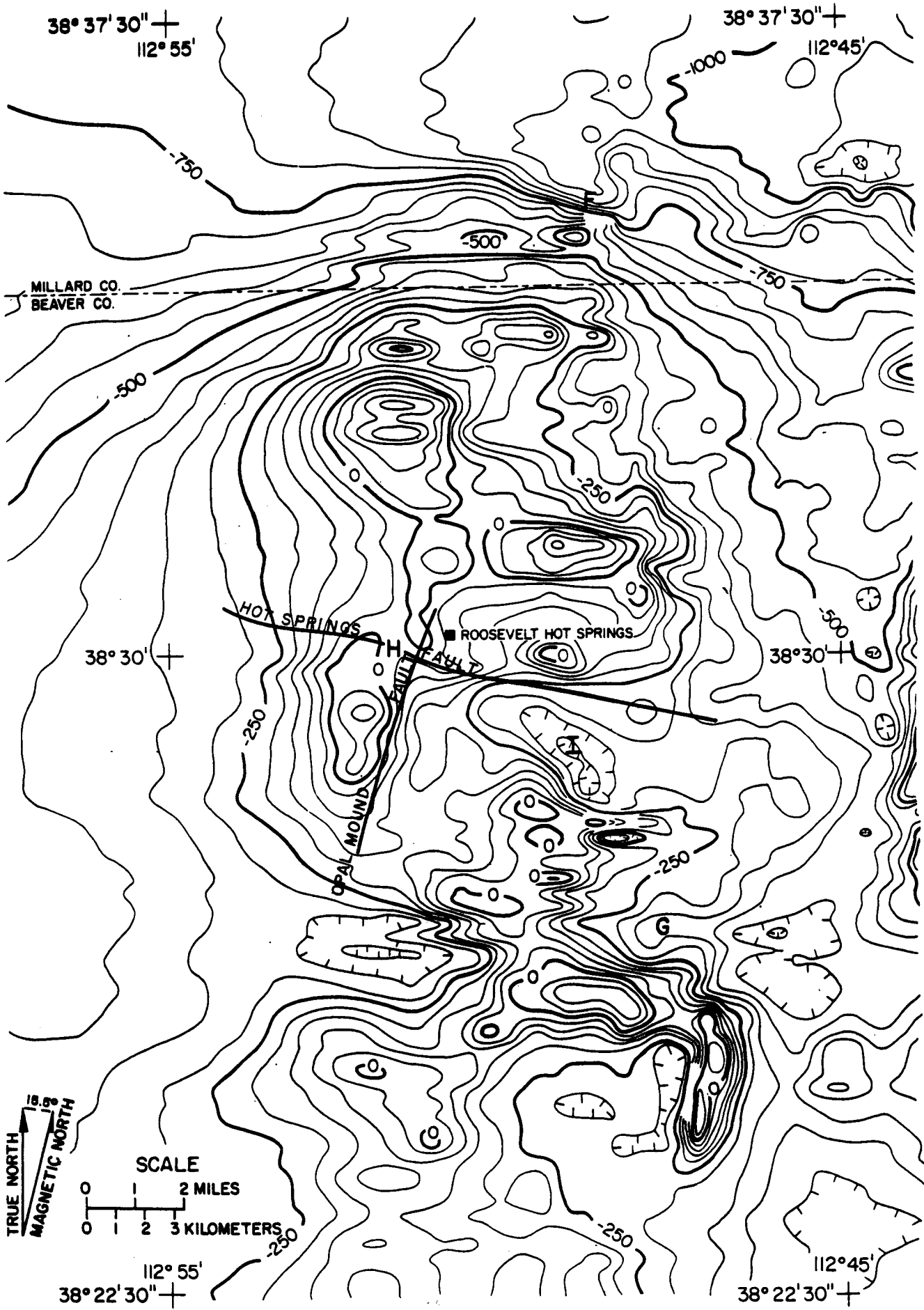Sykes, L. R., 1970, Earthquake Swarms and Seafloor Spreading: J. Geophys. Res., v. 75, p. 6598-6611.
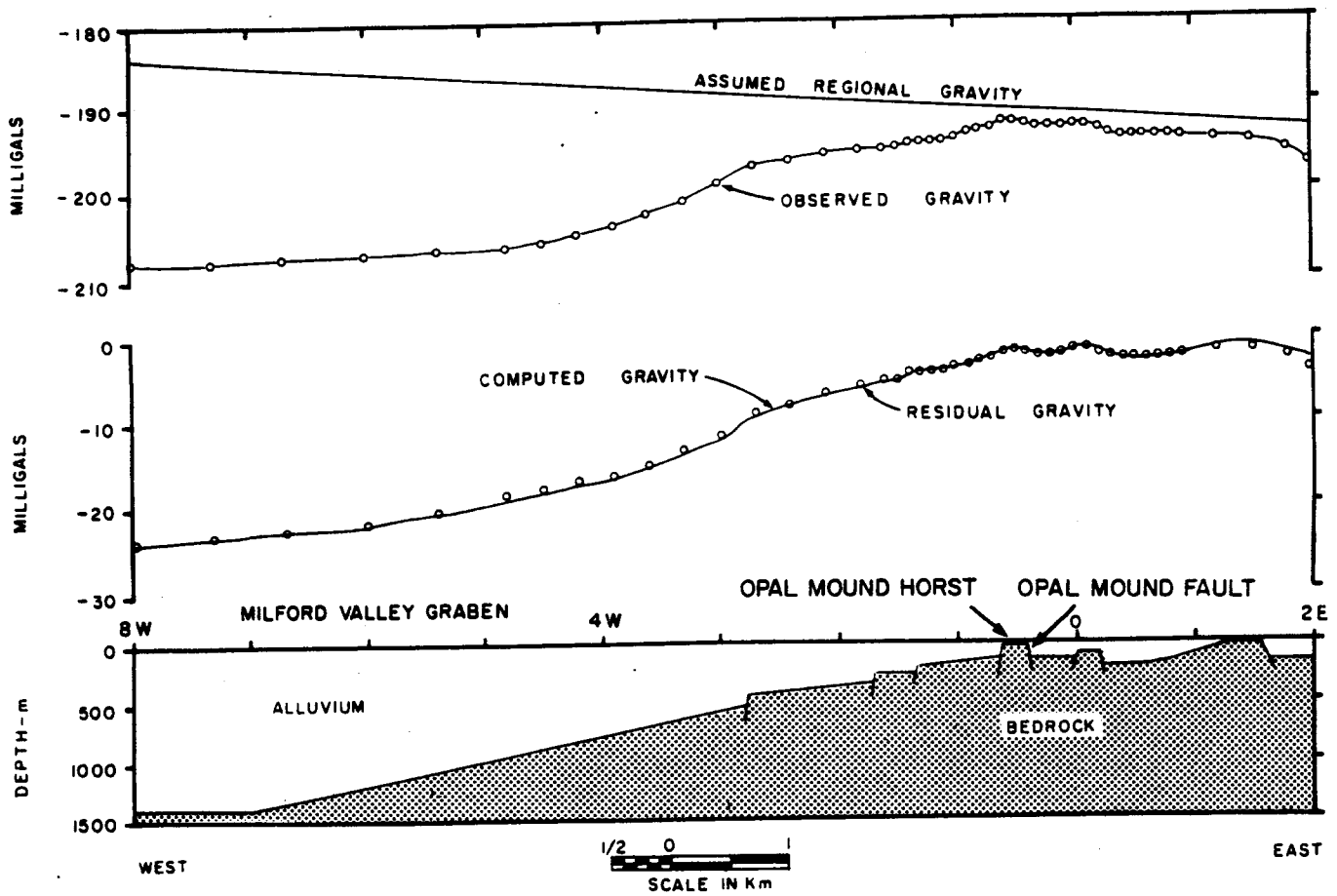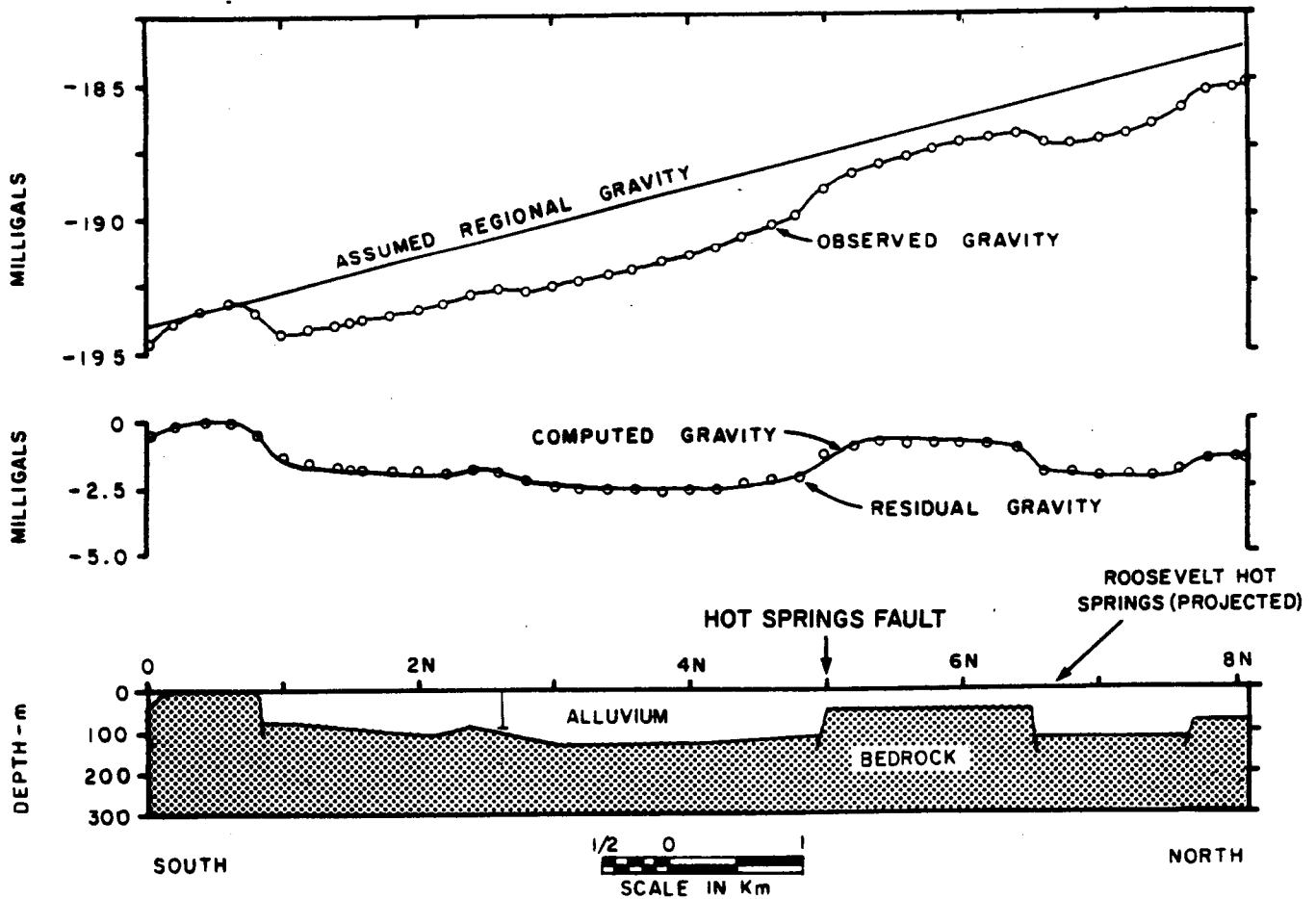
Figure 1

Figure 2

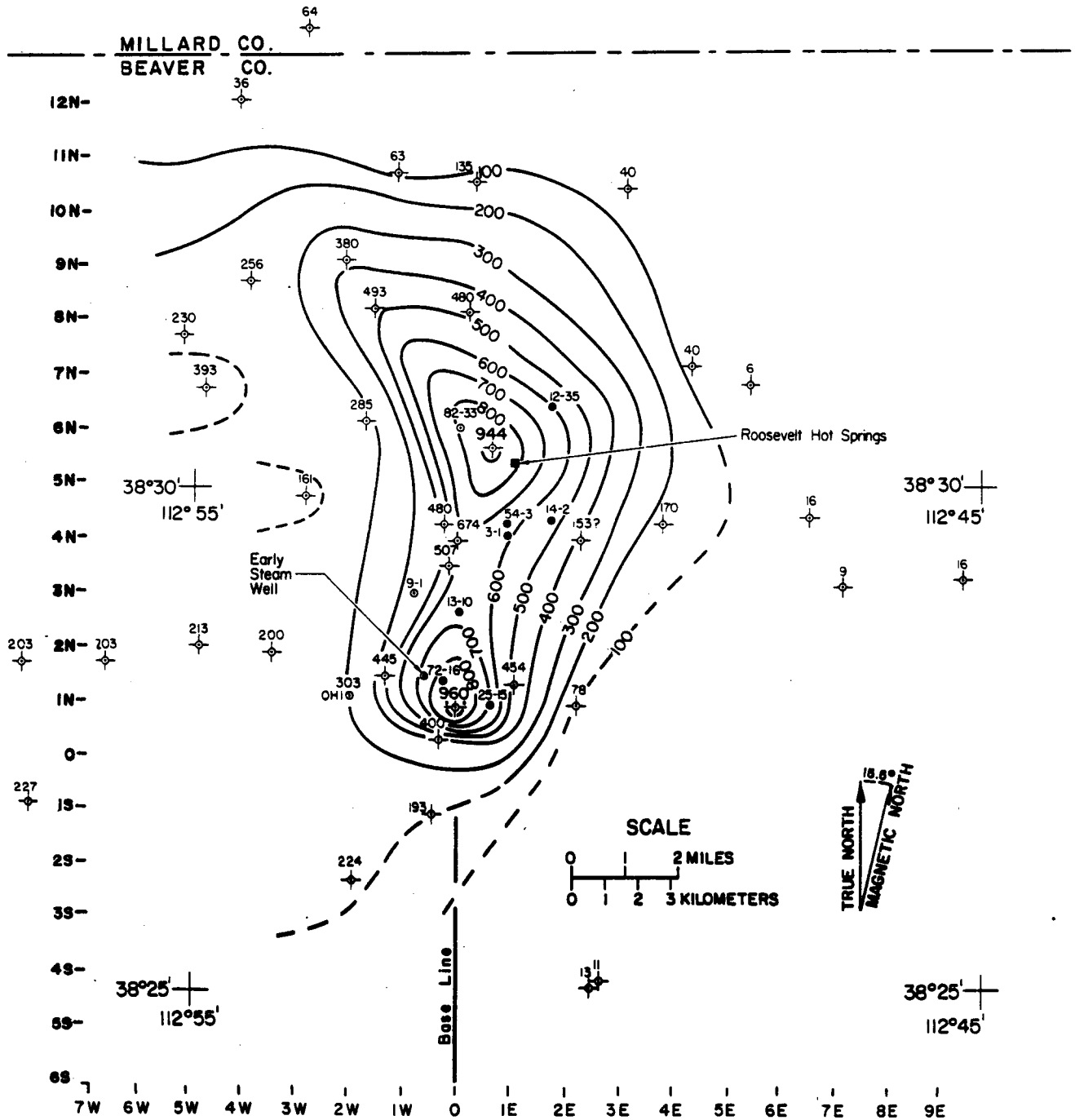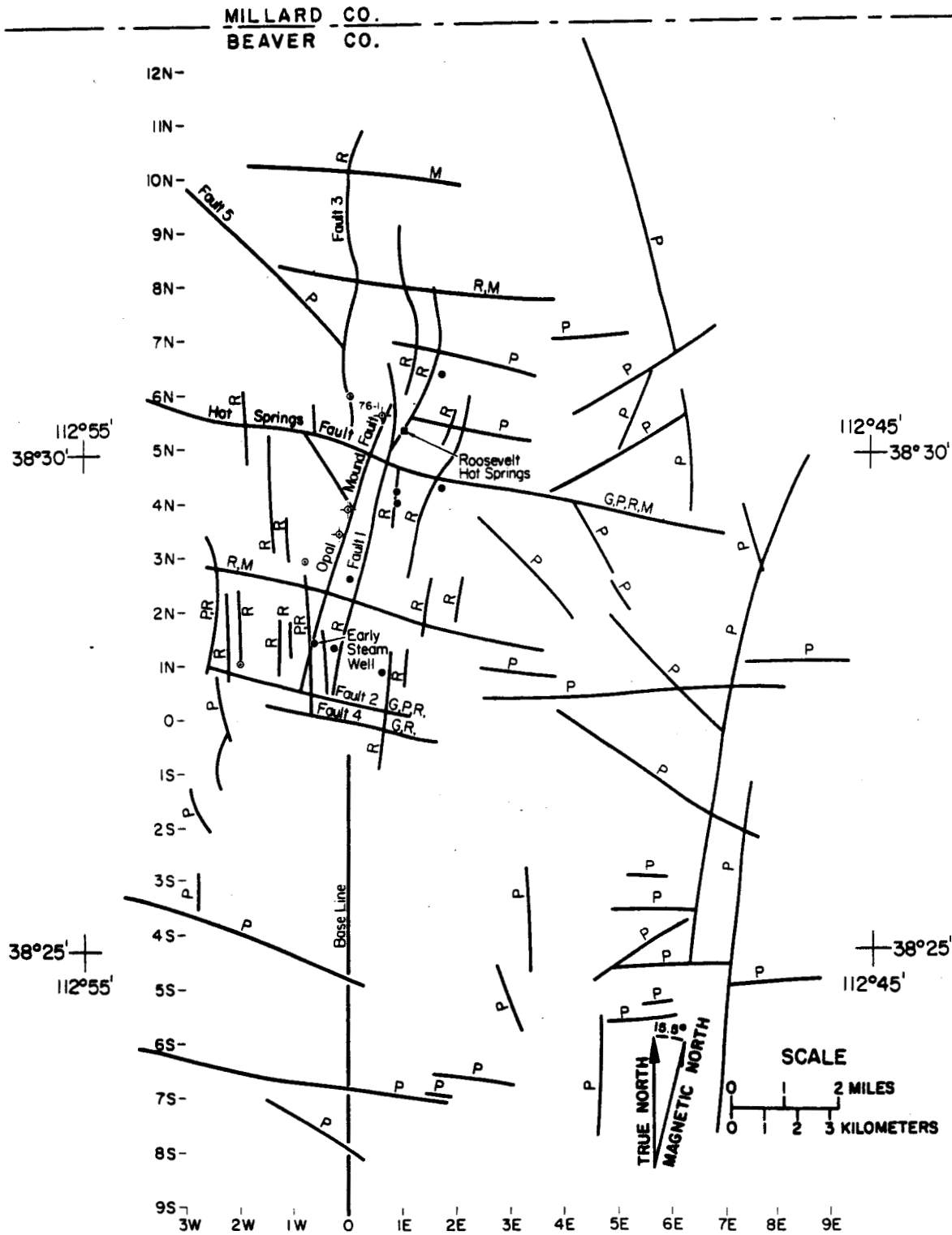Figure 3

Figure 4

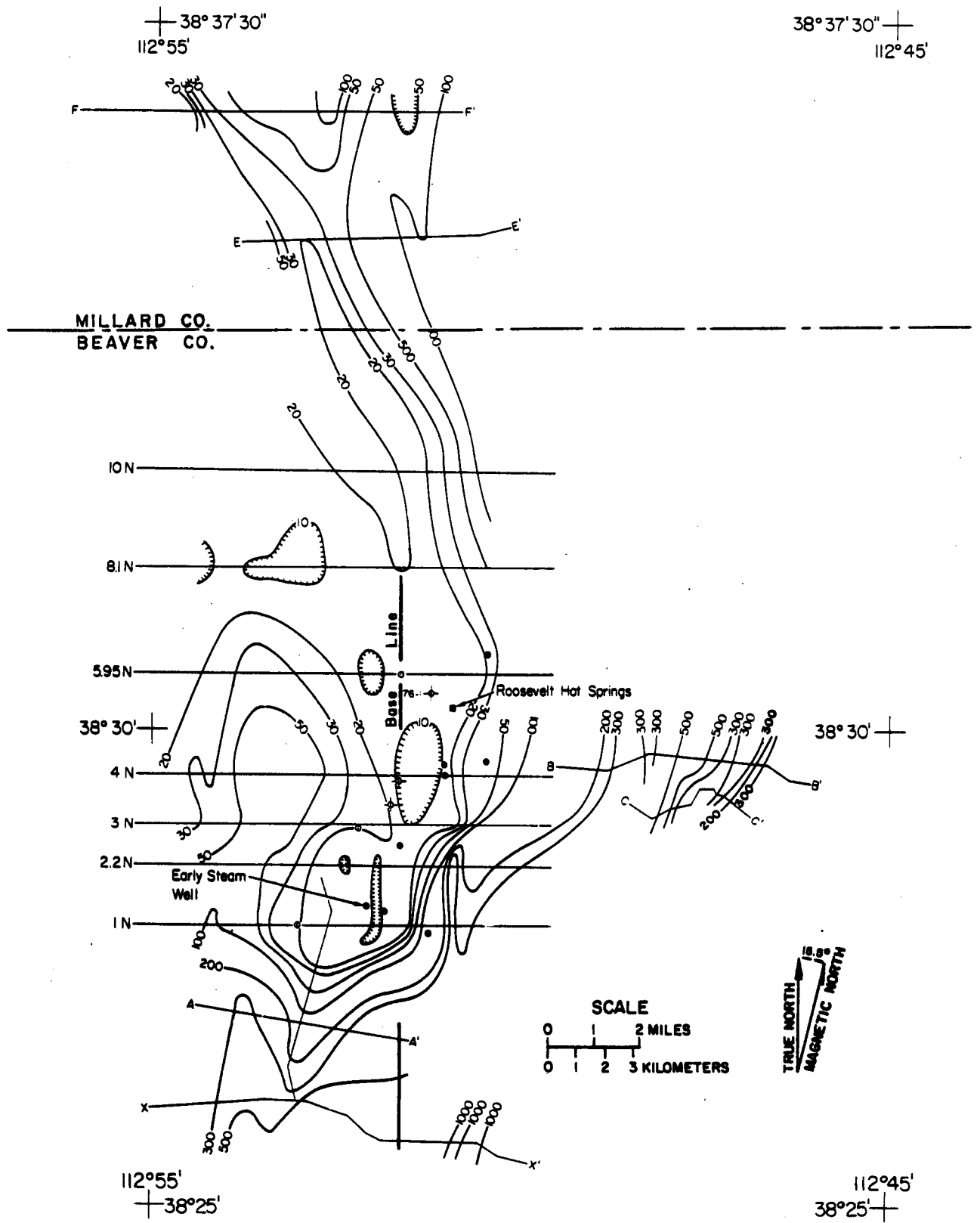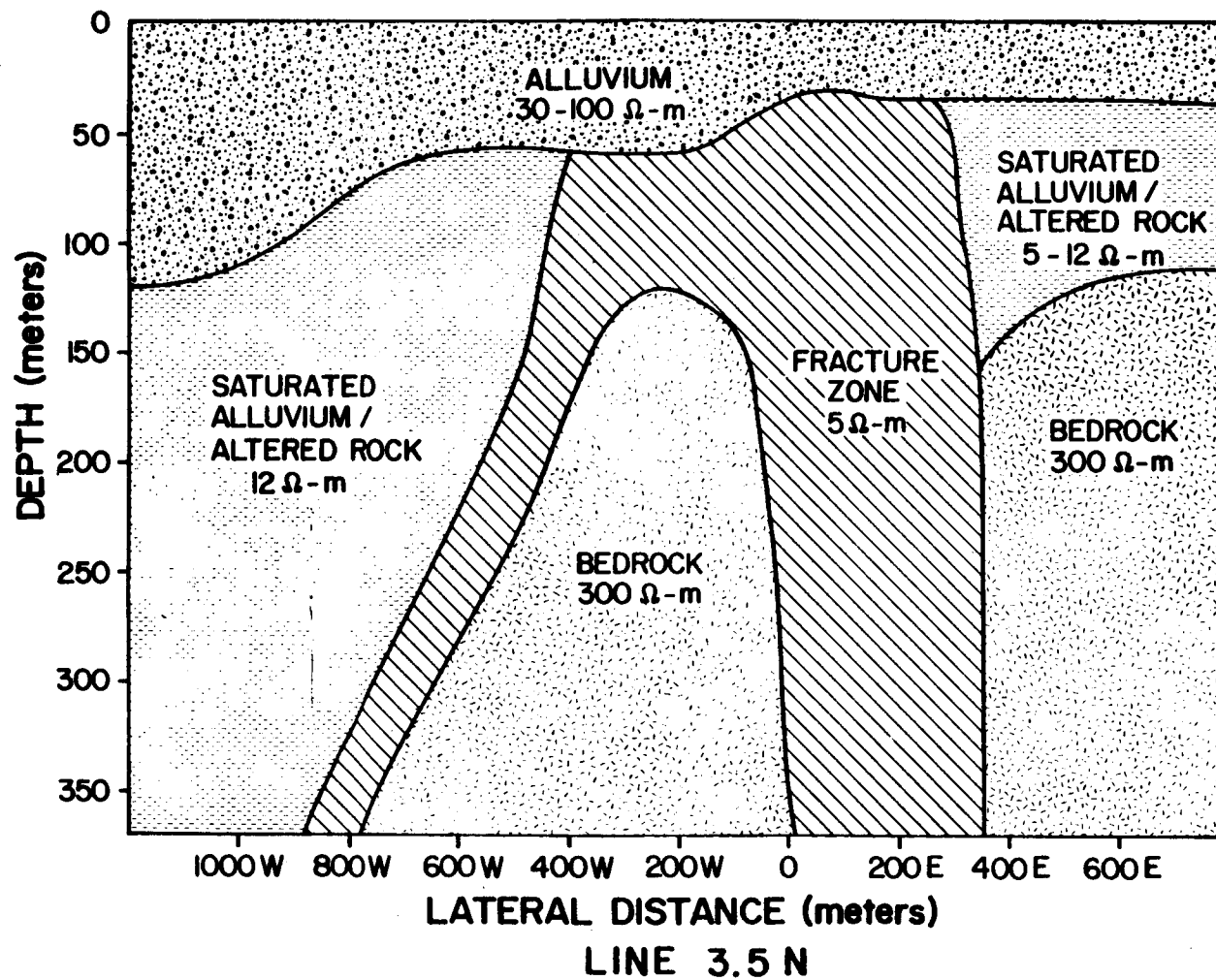Figure 5

Figure 6

Figure 7

Figure 8

Figure 9

ROOSEVELT HOT SPRINGS AREA FIELD TRIP

by

W. T. Parry, W. P. Nash, S. H. Ward

Department of Geology and Geophysics

University of Utah, Salt Lake City, Utah 84112

ROOSEVELT HOT SPRINGS AREA FIELD TRIP

W. T. Parry, W. P. Nash, S. H. Ward

Road Log - Field Trip to Roosevelt Hot Springs Thermal Area via Beaver and Milford with an overnight stop in Beaver. The entire route can be negotiated in 2-wheel drive vehicles, but conventional sedans are not recommended.

The route may begin in Provo, but the mileage origin is the intersection of the Provo University Avenue on-ramp to Interstate-15.

First Day Road Log

Mileage

0   Provo University Avenue - I-15 on-ramp observe Bonneville shore lines, triangular facets and Utah Lake.

5.2 Spanish Fork exit continue on I-15. Good exposure of triangular facets on left. The Escalante route followed Spanish Fork Canyon on the left and entered Utah Valley about here.

17.2 Santaquin exit. Continue on I-15. East Tintic Mountains, East Tintic Mining District and geothermal area on far right. The return trip will provide a better view (daylight permitting).

21.6 Highway road cut in the toe of an ancient landslide.

24.8 Three prominent peaks of Mt. Nebo on the left.

Nebo thrust fault is exposed with

Pennsylvanian and Permian thrust on top of

Jurassic. Young Wasatch Fault Scarp at 10:00

31.2 Another superb exposure of a Recent Wasatch Fault scarp.

32.0 Temporary end of I-15 - caution, two-way traffic.

35.2 Nephi marks the southern end of the Wasatch Mountains. The Gunnison Plateau appears on the left. Mining operation in Jurassic gypsum deposits at 9:00.

56.9 Canyon Mountains in right distance.

81.4 Pavant Butte, a young volcanic cone, in right distance.

Pavant Butte is a 300m high tuff cone, constructed upon a floor of basalt and erupted through Lake Bonneville sometime between 125,000 and 30,000 years ago (Hoover, 1974). The lower sequence consists of black sideromelane tuff which is overlain by brown palagonite tuff. Flows from this field extend southward to within 12 km west of Fillmore where they are overlain by the very young Ice Springs basalt flow.

93.3 Fillmore exit. Take this exit then turn left in to Fillmore.

94.2 Enter Fillmore - Utah's first State Capitol.

94.7 Pass the rest stop and turn right on Utah Highway 100 to Flowell.

This is a good opportunity to fill the fuel tanks in the vehicles. If refueling is necessary, continue into Fillmore, purchase fuel and rendezvous at the rest stop. Mileage does include a refueling stop.

95.2 Buy gasoline.

95.5 Return to rest stop, turn left (west) on Utah 100 to Flowell.

100.0 Junction - continue straight west to Flowell. Ice Springs basaltic andesite flow and cinder cone ahead on left.

101.9 Turn left on paved road and head south.

102.9 Turn right still on paved road. Ice Springs Cone dead ahead, flow on right.

104.8   Junction - take left fork and parallel the edge of the Ice Springs basalt flow.

105.5   Bear left around lava flow.

106.8   Stop #1.   Ice Springs lava flow.

This field is the youngest in the region. The flows are unweathered, and what little vegetation exists grows on portions of windblown material. It overlies Lake Bonneville deposits and must be less than 4,000 to 1,000 years old. A Carbon-14 date on root material in soil under the flow gives an age of 660 ± 170 years B.P. (Valastro and others, 1972). If this age is correct, it makes the Ice Springs field one of the youngest basalt flows in the interior of the United States. There are three major and six subsidiary vents in the field which have erupted a fine-grained basalt which grades from pahoehoe near the field center to aa at the margins. White Mountain, a young rhyolite dome is in the distance to the south. Tabernacle Hill and flows can be seen to the southwest. They are post-Bonneville in age (<12,000 years).

106.9   Bear left to White Mountain

108.5   Stop #2.   White Mountain

This unassuming hill is the youngest rhyolite yet dated in Utah, 0.4 m.y. It is younger than the rhyolites at Roosevelt Hot Springs, but its original morphology has been modified by Lake Bonneville. Obsidian crops out near the base and crystalline rhyolite is exposed along the summit. The pumiceous carapace has been stripped by the waters of Lake Bonneville and gravel deposits consisting predominantly of rhyolite have been formed on the southeast margin of the dome and can be seen as we drive towards the community of Meadow.

108.9 Continue south on gravel road - around the east side of White Mountain.

111.8 Junction - Meadow Hot Springs to the southwest bear left to the town
of Meadow.

114.1 Pavement begins.

114.3 Stop sign. Stop then turn left.

114.8 Turn left again and re-enter I-15 south.

122.0 Black Rock volcano on left.

This is the largest of several vents in the Kanosh volcanic field
which pre-dates Lake Bonneville; Hoover (1974) gives an average date
of 670,000 years B.P.

124.2 North and South Twin Peaks at 2:00 on right.

These are large rhyolite domes, the second of which has been dated at
2.3 m.y. (Lipman and others, 1978).

137.0 Cinder cone of the Cove Fort basaltic-andesite field.

140.2 Junction I-70 continue on I-15 south.

141.2 Sulfurdale. Sulfur mine on left in foothills.

154.7 Mineral Mountain Range in right distance. Northern high point is Bear-
skin Mountain rhyolite dome. Tushar Mountains and Mt. Belknap on left.

159.5 Beaver exit. Take Beaver exit. Night in Beaver.

Second Day Road Log

Following a refreshing night's rest and a gourmet breakfast at the
Ponderosa, rendezvous at the little park near the Beaver Post Office at
the junction of the Beaver Main Street and Utah Highway 21 West.

Mileage

0 Turn west on Utah-21 to Milford. Mineral Mountains ahead and to the
right. Note granitic pluton with white skarn zone in Paleozoic limestone
(Kiabab) at the base of the mountains at 2:00.

4.7 Tertiary volcanics ahead forming southern part of Mineral Range.

11.8 7.6 million year old basalts.

14.5 Paleozoic sediments on right. Kiabab and Coconino. Radium (Dotsons) hot springs on left on Beaver R.

16.4 Minersville turnoff - continue straight to Milford. Sevier River Formation. Thermo Hot Springs to the southwest.

28.8 Stop again. Cross RR tracks and turn right down Milford Main Street.

29.2 Junction Utah 257 - proceed straight ahead on Utah 257.

31.4 Buwana Mine, a skarn copper deposit, at 9:00 in the Rocky Range.

33.4 Turn right onto gravel road to Roosevelt Hot Springs.

34.6 RR tracks.

36.0 Antelope Point Road Junction, continue straight ahead.

40.5 Turn right on road to the Opal Mound.

41.0 STOP #3. Opal Mound and early steam well.

The Roosevelt Hot Springs Thermal Area was a source of implement grade obsidian for the Indians, and opal for lapidarists. Other minerals prompted the first drilling. Hot water was encountered at 24 m in 1967 in a drill hole on the Opal Mound. A drill hole 100 m east of the Opal Mound (the early steam well) encountered hot water which flashed to steam at 50 m and blew out at 81 m requiring 2 months to regain control. Active geothermal exploration began in 1972 resulting in discovery of the potentially commercial thermal reservoir by Phillips Petroleum Co. in 1975.

The Opal Mound consists of opal and chalcedony produced as a result of primary deposition of silica on broad spring aprons. Microbanded, knobby, and colloform opal textures are common. Laminae dip steeply

to vertically within old spring vents exposed along the Opal Mound Fault. Sinter cemented alluvium surrounds the spring vents and constitutes a transition between spring deposits and altered alluvium.

The thermal gradient anomaly map outlines the maximum dimension of the geothermal field as it is currently conceived. Heat flow is probably dominated by convection along three fracture sets trending north-south, east-west, and northwest-southeast. The Opal Mound Fault is one of the north-south set; the deep coves along the range front are believed to be caused by east-west faulting. While high thermal gradients occur west of the Opal Mound Fault, three wells drilled there are all non-productive. From the Opal Mound Fault eastward for 500 m the resistivity data suggest a broad fracture zone; the highest heat flow values occur along this trend in the southern half of the field.

A gravity saddle centers on Ranch Canyon where the geothermal system seems to terminate according to resistivity and thermal gradient data. A low density intrusive beneath the saddle is a possibility. An aeromagnetic survey reveals that the Precambrian (?) rocks to the west of the Opal Mound Fault are right laterally offset by the east-west Hot Springs Fault. Two east-west faults, two kilometers south of the early steam well downthrow the geothermal system to the south.

An AMT/MT survey has defined an anomalous zone in the vicinity of the geothermal system.

41.6 Opal Mound fault on left roadside with exposed Precambrian boulders.

42.2 Phillips 13-10 production well.

42.8 Turn left from main gravel road to Phillips 54-3 and 3-1.

43.4 STOP #4. Phillips Geothermal well 54-3.

Phillips Petroleum Company's well 3-1 and the twin 54-3 are the discovery wells for the Roosevelt Hot Springs thermal reservoir. Seven producing wells have been drilled; maximum depth is 2600 m and potential fluid production per well averages 4.5×10^5 kg/hr at a temperature greater than 260°C.

The thermal water is relatively dilute sodium chloride brine (total dissolved solids 7,000 to 8,000 mg/l). Chemical thermometers applied to the waters indicate quartz temperatures from 140°C for the modern surface seep to 283°C for water produced from the thermal reservoir and Na-K-Ca temperatures from 239°C for the surface seep to 286°C for water produced from the deep reservoir.

Continue north on dirt road.

43.8 Turn left down Hot Springs Wash on jeep road.

44.1 STOP #5. At site of Historical Cabin.

Altered and cemented alluvium is the dominant rock type which crops out in the Roosevelt thermal area. Cemented alluvium consists of mineral and rock fragments derived from gneiss, granitic rocks, and volcanic rocks of the Mineral Mountains which have been cemented by opal and chalcedony. The feldspars have been altered by acid-sulfate water to alunite, opal, and hematite. Native sulfur occurs with sinter and in intergranular spaces in cemented alluvium. Return to vehicle, turn around. Return to dirt road, turn left to Roosevelt Resort.

44.7 STOP #6. Resort Area.

The spring discharge was 38 1/min at 88°C in 1908, 4 1/min at 85°C in 1950, "small" at 55°C in 1957 and in 1966 the spring was completely dry. Only a small seep at 25°C located 500 m northwest occurs today.

As we look northwest from here our eye will follow an inferred fault mapped by resistivity and photogeology. This inferred fault follows the axis of the thermal gradient anomaly in this northern half of the system. The system has been tested northwest of here only by well 82-33 which lies southwest of the inferred fault. It is possible that leakage of brines northwestward accounts for the thermal gradient high but it is equally possible that the convective system extends north-westward. Resistivity and thermal gradient data both indicate that the system is leaking brine to the west via the northwest-southeast and east-west fracture sets.

45.1 STOP #7. Salt Spring.

Lunch

Altered rocks have been sampled in the subsurface in three shallow core-drill holes; DDH 76-1 was drilled on the ridge of cemented alluvium 100 m southwest of Stop 7. Altered and cemented granitic alluvium were encountered from 3 m to 20 m. Detrital fragments of quartz and feldspar are cemented by opal and chalcedony. The feldspars have been altered to opal, alunite, jarosite, kaolinite, and muscovite. Biotite is altered to vermiculite. Intensely altered quartz monzonite occurs from 20 m to 32 m. Vermiculite, kaolinite, muscovite, interstratified montmorillonite-muscovite, opal, and chalcedony occur as fracture fillings, patches, and

replacement of feldspars. The interval 32 m to 36 m is fault gouge and breccia consisting of quartz in a matrix of montmorillonite and muscovite with veinlet and disseminated pyrite. Moderately altered quartz monzonite occurs from 36 m to the total depth of 61 m and contains veinlets of green muscovite, chlorite, pyrite, and scattered calcite.

Turn around and retrace route back past Phillips 54-3 to main gravel road.

46.7 Turn left on main gravel road.

47.2 Turn right on dirt road.

47.9 STOP #8. Bailey Ridge flow.

This rhyolite flow has been dated at 0.79 m.y. It is virtually non-porphyritic and extremely fluid in aspect compared to most rhyolite flows. It is chemically and morphologically similar to a flow in Wild-horse Canyon, 5 km to the south. The massive obsidian in this flow has provided excellent artifact grade material.

48.5 STOP #9. Schoo Mine. Careful of treacherous rubble and mine faces.

The perlite mine exposes the upper portion of the Bailey Ridge rhyolite flow. With the exception of a layer of massive obsidian at the floor of the workings, the flow consists of dense to frothy perlite. A relatively thin soil is developed on the surface of the flow. Return to main gravel road.

50.5 Turn left (south) on dirt road.

51.3 Lower mountain on left is Big Cedar Cove rhyolite dome.

51.8 Phillips geothermal well 25-15.

53.2 Wildhorse Canyon flow - cliffs of obsidian at 8:00 to the rear left. On skyline left are 3 coalescing rhyolite domes.

54.2 Turn left on Lower Ranch Canyon road. Drive through Mineral Mountains granitic pluton.

56.9 Right turn at junction, then left.

57.3 STOP #10. Pumice Hole Mine.

Air-fall and ash-flow tuffs are exposed here. To the north and east are three rhyolite domes which post-date the pyroclastic eruptions.

The paleotopography was rugged, probably quite similar to the present topography. Pyroclastic eruptions preceeded formation of the domes filling the valley now occupied by Ranch Canyon. At the Pumice Hole mine the lowermost exposed deposits are air-fall tuffs. These are overlain by several ash-flow tuffs which were emplaced at moderately low temperatures and are unwelded.

57.5 Turn left on upper Ranch Canyon road. Drive through Mineral Mountains granitic pluton.

60.6 Corral Canyon.

60.9 Conical dome in foreground at 4:00 is Corral Canyon rhyolite.

63.5 Bear right to Pass Road to Milford.

69.8 Milford - leave for Delta on Utah 257.

92.7 Black Rock Basalts to east. Further east lie rhyolites of the Cove Creek region which have been dated at 2.3 m.y.

100.7 Cove Creek rhyolite east at 4:00.

120.7 Dannenburg Butte to west. Quaternary basalt with Bonneville terraces. Pavant Butte at 2:00 east.

124.3 Sunstone knoll.

124.7 Quaternary Deseret basalt flow on left.

138.2 Right turn on US 6/50 to Delta.

142.3 Bear left on US 6/50.

150.7 Crater Hot Springs KGRA 30 km to west.

191.2 Main Tintic Mining District town of Eureka.

195.7 East Tintic Mining District. Bergin Mine and KGRA at 2:00.

201.1 Elberta - proceed east to I-15 at Santaquin and then north to starting
       point.

REFERENCES

Hoover, J. D., 1974, Periodic Quaternary volcanism in the Black Rock Desert, Utah: <u>Brigham Young Univ. Geol. Studies</u>, v. 21, p. 3-72.

Lipman, P. W., Rowley, D. D., Mehnert, H. H., Evans, S. H., Jr., Nash, W. P., and Brown, F. H., 1978, Pleistocene rhyolite of the Mineral Mountains, Utah - geothermal and archeological significance: <u>Jour</u>. <u>Res</u>. <u>U</u>. <u>S</u>. <u>Geol</u>. <u>Surv</u>., in press.

Valastro, S., Jr., Davis, E. M., and Valera, A. G., 1972, University of Texas at Austin Radiocarbon Dates IX: <u>Radiocarbon</u>, v. 14, no. 2, p. 461-485.